JOURNAL OF PETROLOGY

Journal of Petrology, 2015, Vol. 56, No. 7, 1251–1284
doi: 10.1093/petrology/egv029
Advance Access Publication Date: 29 July 2015
Original Article

OXFORD

Can Fractional Crystallization, Mixing and Assimilation Processes be Responsible for Jamaican-type Adakites? Implications for Generating Eoarchaean Continental Crust

A. R. Hastie[1,2]*, J. G. Fitton[2], S. F. Mitchell[3], I. Neill[4,5], G. M. Nowell[4] and I. L. Millar[6]

[1]School of Geography, Earth and Environmental Sciences, University of Birmingham, Edgbaston, Birmingham B15 2TT, UK, [2]School of GeoSciences, University of Edinburgh, King's Buildings, Edinburgh EH9 3JW, UK, [3]Department of Geography and Geology, University of the West Indies, Mona, Kingston 7, Jamaica, [4]Department of Earth Sciences, Durham University, South Road, Durham DH1 3LE, UK, [5]School of Geographical and Earth Sciences, Glasgow University, Gregory Building, University Avenue, Glasgow G12 8QQ, UK and [6]NERC Isotope Geoscience Laboratories, Keyworth, Nottingham NG12 5GG, UK

*Corresponding author. Telephone: +44 (0)121 4144178. E-mail: a.r.hastie@bham.ac.uk

Received July 3, 2014; Accepted May 15, 2015

ABSTRACT

Understanding how the Earth's first continental land masses were generated is important because the processes responsible directly affected the evolution of the planet's primordial silicate interior, and also its atmosphere and hydrosphere. Archaean continental crust is dominated by rocks of the trondhjemite–tonalite–granodiorite (TTG) suite. These can be divided into (1) a mid- to late Archaean (~3·5–2·5 Ga) suite with low SiO_2 and high MgO, Sr and transition element contents, and (2) an Eoarchaean (>3·5 Ga) suite with higher SiO_2 and lower MgO, Sr and transition element concentrations. Cenozoic adakites are considered to be compositionally similar to mid- to late Archaean (~3·5–2·5 Ga) TTGs, but not the oldest TTG rocks. Conversely, a suite of Early Eocene adakite-like rhyodacites (Jamaican-type adakites: JTA) from Jamaica are shown to be geochemically similar to the Eoarchaean TTGs. In contrast to newly discovered JTA-like rocks (Ryozen low Sr/Y) in Japan, new trace element and Nd–Hf radiogenic isotope data in this study confirm that the Jamaican JTA cannot be formed by complex mixing, assimilation and fractional crystallization processes. New partial melt models here explore several different source compositions (mid-ocean ridge basalt, ocean island basalt and oceanic plateau), mineral modes, melt modes and partition coefficients. The results of these models clearly demonstrate that the JTA and the Eoarchaean TTG can be generated by partial melting of plagioclase- and garnet-bearing amphibolite source regions with oceanic plateau-like compositions. Further modelling shows that the JTA and Eoarchaean TTG low MgO and transition element abundances can be derived from two dominant processes: (1) relatively shallow partial melting of subducting oceanic crust (compositionally similar to Mesozoic oceanic plateau basalt) whereby the slab melts ascend without interacting with a mantle wedge; (2) partial melting of oceanic plateau-like subducting oceanic crust followed by interaction of the slab melts with a thin and/or discontinuous (boudinage-like?) mantle wedge whereby the expected increase of MgO, Ni, and Cr in the slab melts is obliterated by fractional crystallization of ferromagnesian minerals (mostly amphibole). Consequently, using the JTA as a modern analogue for Eoarchaean TTG production, we propose the existence of subduction zones consuming oceanic plateau-like oceanic crust in Eoarchaean times.

Key words: early Archaean (Eoarchaean) continental crust; high-Nb basalts; Jamaican-type adakite (JTA); mantle metasomatism; oceanic plateau subduction; trondhjemite–tonalite–granodiorite (TTG)

INTRODUCTION

The processes responsible for generating the continental crust have resulted in the modification of the Earth's mantle, hydrosphere and atmosphere throughout geological time. However, the generation and subsequent evolution of the Earth's oldest (>3·5 Ga) continental crust are poorly understood and are currently hotly debated (e.g. Hoffmann *et al.*, 2010, 2011; Polat, 2012, 2013; van Hunen & Moyen, 2012; Bédard *et al.*, 2013; Ziaja *et al.*, 2014; Rollinson, 2014; Turner *et al.*, 2014). The oldest surviving continental rocks are the Acasta gneisses, Canada (~4·0 Ga) (Bowring *et al.*, 1990) and, although Archaean crust can have a varied lithology depending on its age (e.g. Kusky & Polat, 1999), the majority (estimates up to ~90%) of the early continental crust from 4·0 to 3·5 Ga is composed of variably deformed Na-rich granitoids of the trondhjemite–tonalite–granodiorite (TTG) rock suite that are considered to be derived from the partial melting of metabasic source regions (e.g. Barker & Arth, 1976; Rapp et al., 1991; Rapp & Watson, 1995; Martin, 1999; Clemens *et al.*, 2006; Moyen & Stevens, 2006; Nutman *et al.*, 2009; Friend & Nutman, 2011; Nagel *et al.*, 2012; Polat, 2012). Nevertheless, the composition and tectonic setting of this basaltic source region remain controversial (Martin, 1999; Foley *et al.*, 2002; Hoffmann *et al.*, 2011; Adam *et al.*, 2012; Laurie & Stevens, 2012; Moyen & van Hunen, 2012; Nagel *et al.*, 2012; Polat, 2012; Zhang *et al.*, 2013; Ziaja *et al.*, 2014).

Hastie *et al.* (2010*a*) described a suite of Early Eocene rhyodacites from Jamaica (Fig. 1), called the Newcastle Volcanics, which have very similar compositions to Eoarchaean TTG suites. Data suggested that the Newcastle Volcanics were generated by partial melting of a subducting portion of an oceanic plateau. The Newcastle Volcanics were subsequently used as a modern analogue of Eoarchaean TTG suites and Hastie *et al.* (2010*a*) proposed that Early Archaean continental rocks are derived from the subduction of oceanic plateau-like subducting plates on the early Earth. However, recently, other Newcastle Volcanics-like rocks have been described from other parts of the world and their petrogenesis has been explained by fractional crystallization processes without the need for oceanic plateau-like metabasic protoliths (Shuto *et al.*, 2013). In addition, although it is gaining support, the use of the Newcastle rocks as modern analogues of Eoarchaean TTG has proved controversial (e.g. Castillo, 2012; Moyen & Martin, 2012). Consequently, the purpose of this contribution is to (1) use new geochemical data to investigate possible fractional crystallization, mixing and assimilation processes for generating the Newcastle Volcanics, surrounding arc rocks and high-Nb basalts on Jamaica in a single geochemically coherent model, and (2) further discuss the petrogenesis of the Newcastle samples and the implications for the potential composition of the Eoarchaean continental source protolith and tectonic environment.

As a result of the controversy surrounding the petrogenesis of the Newcastle rocks, we use a relatively large number of geochemical models to study the latter and make use of extensive Supplementary Data (available for downloading at http://www.petrology.oxfordjournals.org) to present all the modelling parameters used, the rationale for their use, and to display the results of the calculations. Specifically, we have used published experimental results to constrain modelling parameters using standard mass-balance procedures—similar to other studies (e.g. Moyen & Stevens, 2006).

JAMAICAN GEOLOGY

The geology of Jamaica is dominated by Tertiary limestones and recent alluvial deposits (Mitchell, 2004, 2013). In contrast, a third of the island exposes Cretaceous inliers predominantly composed of island arc rocks (Fig. 1a and b) (e.g. Mitchell, 2006). In the east, there is the NW–SE-trending Wagwater Belt, which is an inverted Paleogene extensional basin (Fig. 1c; Supplementary Data Fig. A1, Appendix A) (Jackson & Smith, 1978). The Wagwater Belt contains volcanic rocks that include the Early Eocene Newcastle Volcanics (the Jamaican-type adakites; JTA) and the Halberstadt Volcanics (associated high-Nb basalts) (Jackson & Smith, 1978; Jackson *et al.*, 1989).

Here, new data are presented from the Newcastle and Halberstadt Volcanics and island arc lavas in the surrounding Cretaceous inliers (Fig. 1b; Supplementary Data Tables B1–B4, Appendix B). The island arc rocks studied consist of the following: (1) the tholeiitic to calc-alkaline (Hauterivian–Aptian) Devils Racecourse Formation (Benbow Inlier) (Hastie *et al.*, 2009; Brown & Mitchell, 2010); (2) the predominantly calc-alkaline igneous rocks (early to mid-Campanian) of the Central Inlier (Hastie *et al.*, 2013; Mitchell, 2013); (3) a granodiorite pluton (the Above Rocks Granodiorite) and associated lava flows (the Mount Charles and Border Volcanics) in the Above Rocks Inlier; (4) porphyritic, calc-alkaline lavas of the Thornton Formation (early to mid-Campanian) from the Sunning Hill Inlier; (5) porphyritic island arc tholeiite lavas of the Bellevue Formation (mid- to late Campanian) in the Blue Mountains Inlier (Mitchell & Ramsook, 2009; Hastie *et al.*, 2010*c*) (Fig. 1b; Supplementary Data Figs A2–A4, Appendix A).

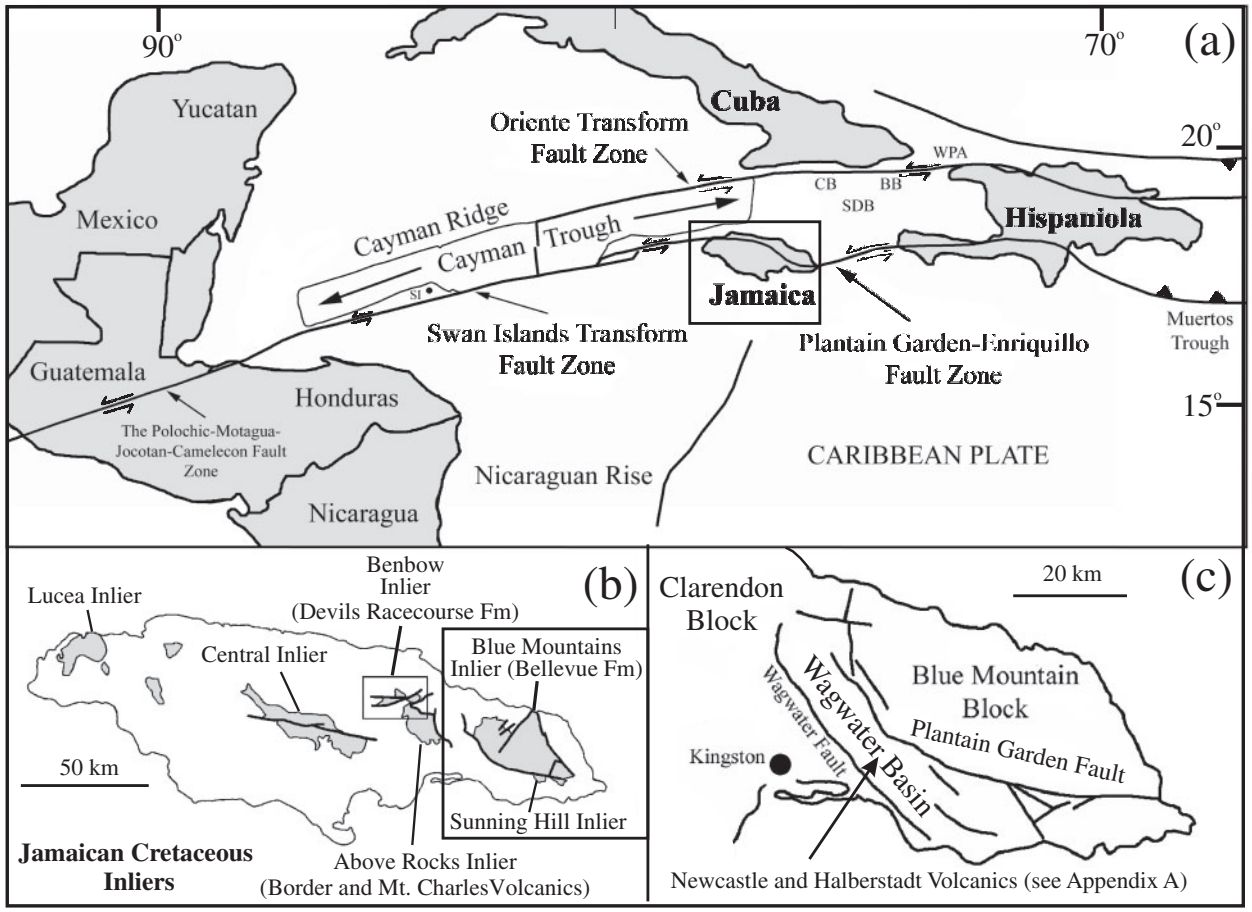

Fig. 1. (a) Location map for Jamaica and the Caribbean–North American plate boundary. BB, Baitiquiri Basin; CB, Chivirico Basin; SDB, Santiago Deformed Belt; SI, Swan Islands; WPA, Windward Passage Area. (b) Location map showing the Cretaceous inliers and the main volcanic island arc successions of Jamaica [modified from Lewis & Draper (1990)]. (c) Location of the Newcastle and Halberstadt Volcanics in the Wagwater Basin, Eastern Jamaica. More detailed maps can be found in Supplementary Data Appendix A.

CLASSIFICATION AND PETROGENESIS OF TTGS AND ADAKITES

Early Archaean (>3·5 Ga) versus Mid- to Late Archaean (<3·5) TTGs

Archaean TTG plutons are commonly composed of quartz, Na-rich plagioclase, amphibole, biotite, Fe–Ti oxides, apatite, epidote, allanite, titanite and zircon (e.g. Jahn *et al.*, 1981; Drummond *et al.*, 1996; Martin *et al.*, 2005; Moyen & Stevens, 2006; Hoffmann *et al.*, 2011). Only the high-Al (>15 wt % Al_2O_3) TTG group will be considered here because it has compositions analogous to the Newcastle Volcanics (Barker *et al.*, 1976; Barker & Arth, 1976; Hastie *et al.*, 2010*a*, 2010*b*). These TTG rocks have >64 wt % SiO_2, Al_2O_3 (>15 wt %), high Na_2O of 3·0–7·0 wt %, low K_2O/Na_2O ratios (<0·6) and low Y and Yb contents (<20 and <1·8 ppm respectively) (e.g. Barker & Arth, 1976; Barker *et al.*, 1976; Jahn *et al.*, 1981; Drummond *et al.*, 1996; Smithies, 2000; Condie, 2005; Martin *et al.*, 2005; Nutman *et al.*, 2009; Hoffmann *et al.*, 2011). Importantly, in the literature TTG rocks can be broadly divided into (1) a mid- to late Archaean (~3·5–2·5 Ga) suite with lower SiO_2 and higher MgO, Sr, Ni, Cr, Co and V contents, and (2) an Eoarchaean (>3·5 Ga) suite with higher SiO_2 and lower MgO, Sr, Ni, Cr, Co and V concentrations (Table 1) (e.g. Smithies, 2000; Martin & Moyen, 2002; Smithies *et al.*, 2003; Martin *et al.*, 2005; Willbold *et al.*, 2009; Rollinson, 2014). Experimental petrology and trace element modelling suggest that the Archaean TTG are derived from the fusion of metabasic protoliths that have been transformed into amphibolite, garnet amphibolite or eclogite (e.g. Rapp *et al.*, 1991, 2003; Sen & Dunn, 1994*a*; Rapp & Watson, 1995; Moyen & Stevens, 2006; Zhang *et al.*, 2013).

Cenozoic adakites—a TTG analogue and an Eoarchaean problem?

Modern adakites are intermediate–silicic volcanic and intrusive rocks that contain plagioclase, amphibole, pyroxene, biotite, quartz and several accessory phases (e.g. Defant *et al.*, 1992; Martin *et al.*, 2005). Adakites have SiO_2 >56%, Al_2O_3 > 15%, high Na_2O 3·5–7·5 wt %, MgO < 3%, low K_2O/Na_2O < 0·5, low Y and Yb (<18 and <1·9 ppm respectively), high Ni, Cr and V abundances

Table 1: Average chemical comparison of 'normal' island arc ADR lavas, adakites and TTG suites

	ADR	Adakites					Eoarchaean TTG					Later Archaean TTG			
	Island arc D1996	Cenozoic adakite D1996	High-silica adakites M2005	Adakites C2005	JTA[1] H2010a	Low-silica adakites M2005	3·57–3·86 Ga N2009	3·6–3·8 Ga Hf2010[2]	>3·5 Ga M2005	>3·5 Ga C2005[3]	Mean	2·8–3·0 Ga Hf2010[2]	<3·0 Ga M2005	<3·5–2·5 Ga C2005[3]	Mean
SiO_2	67·72	63·89	64·80	62·43	71·16	56·25	70·50	69·80	69·59	70·47	70·09	68·15	68·36	68·34	68·28
TiO_2	0·49	0·61	0·56	0·67	0·34	1·49	0·29	0·34	0·39	0·30	0·33	0·37	0·38	0·40	0·38
Al_2O_3	15·44	17·4	16·64	17·05	15·69	15·69	15·59	15·83	15·29	15·19	15·48	16·29	15·52	15·48	15·76
Fe_2O_3	4·92[4]	4·67[4]	4·75	3·99	3·15	6·47	2·65[5]	2·85	3·26	2·74	2·88	3·34	3·27	3·53	3·38
MnO	0·11	0·08	0·08	0·08	0·04	0·09	0·04	0·05	0·04		0·04	0·04	0·05	0·06	0·05
MgO	1·48	2·47	2·18	3·31	1·36 (1·29)[6]	5·15	1·02	0·95	1·00	0·96	0·98	1·20	1·36	1·41	1·32
CaO	3·98	5·23	4·63	6·53	1·23	7·69	3·06	3·15	3·03	2·84	3·02	3·74	3·23	3·26	3·41
Na_2O	3·29	4·40	4·19	4·25	5·94	4·11	4·72	4·86	4·60	4·51	4·67	4·50	4·70	4·55	4·58
K_2O	2·95	1·52	1·97	1·42	0·49	2·37	1·58	1·70	2·04	2·36	1·92	1·72	2·00	2·11	1·94
P_2O_5	0·11	0·19	0·20	0·26	0·10	0·66	0·07	0·08	0·13	0·10	0·1	0·09	0·15	0·14	0·13
Sc	10·9	9·1			(6·0)			2·4			2·4	4·7			4·7
V	71	72	95		36	184	26	22	39		29	39	52		45·5
Cr	21	54	41	82	30 (37)	157	15	12	34	58	30	15	50	37	34
Co	19	13			7·1		29·6[7]	4·1			4·1	7·4			7·4
Ni	9	39	20	64	20 (25)	103	22	7	12	17	15	20	21	22	21
Rb	109	30	52	15	6·72	19	64·81		79	81·7	75		67	64·84	66
Sr	229	869	565	1550	129 (135)	2051	298	295	360	362	329	292	541	490	441
Y	28·5	9·5	10·0	9·7	8·3	13	8·3	6·9	12·0	8·2	8·85	7·1	11·0	10·3	9·47
Zr	133·0	117	108·0	117·0	135·3	188·0	124·6	141·3	166·0	156·6	147·1	125·6	154·0	153·4	144·3
Nb	15·80	8·3	6·00	9·70	6·05	11·00	4·27	3·60	8·00	5·26	5·28	4·09	7·00	6·69	5·93
Ba	514	485	721	309	220	1087	260	228	449	511	362	500	847	723	690
La	32·01	17·55	19·2	24·00	13·87	41·10	12·67	18·09	35·3	20·54	21·65	16·72	30·8	33·51	27·01
Ce	55·27	34·65	37·7	65·00	21·05	89·80	22·72	33·20	61·7	36·95	38·64	30·59	58·5	61·07	50·05
Nd	17·85	20·14	18·2	26·00	8·36	47·10	9·48	15·03	25·80	13·32	15·9	12·51	23·20	23·62	19·78
Sm	6·40	3·15	3·4	4·70	1·61	7·80	2·17	2·57	4·20	2·83	2·94	2·19	3·50	4·03	3·24
Eu	3·60	0·97	0·9	1·37	0·54	2·00	0·60	0·69	1·00	0·89	0·79	0·72	0·90	1·03	0·88
Gd	6·99	2·25	2·8	2·30	1·50	4·80	1·64	2·03	3·20	2·33	2·3	1·94	2·30	2·93	2·39
Tb	0·76	0·37		0·40	0·22		0·27	0·27		0·349	0·30	0·27		0·39	0·33
Dy	6·88	1·43	1·9		1·31	2·80	1·35	1·43	1·80		1·53	1·44	1·60		1·52
Er	5·03	0·76	0·96		0·70	1·21	0·74	0·72	0·77		0·74	0·73	0·75		0·74
Yb	4·26	0·91	0·88	0·81	0·71	0·93	0·77	0·71	0·78	0·85	0·78	0·68	0·63	0·86	0·72
Lu	0·47	0·15	0·17	0·09	0·13	0·08	0·12	0·11	0·20	0·14	0·14	0·10	0·12	0·14	0·12
Hf	2·60	3·5		3·30	3·15			3·78		4·53	4·16	3·23		4·26	3·75
Ta	0·49	0·53		0·60	0·50		0·65	0·32		0·34	0·44	0·24		0·80	0·52
Th	4·96	3·52		3·90	2·89		4·04	3·85		1·92	3·27	2·61		7·55	5·08
U	0·67	0·99		1·20	0·96		0·72	0·54		0·71	0·67	0·24		1·53	0·89
Sr/Y	8·04	91·47	56·50	159·79	16·50	157·77	35·9	42·94	30·00	44·15	38·25	41·28	49·18	47·57	46·01
La/Yb	7·51	19·29	21·82	29·63	19·76	44·19	16·45	25·46	45·26	24·16	27·83	24·54	48·89	38·97	37·47
$CaO + Na_2O$	7·27	9·63	8·82	10·78	7·00	11·8	7·78	8·02	7·63	7·35	7·70	8·23	7·93	7·81	7·99

D1996, Drummond *et al.* (1996); M2005, Martin *et al.* (2005); C2005, Condie (2005); H2010a, Hastie *et al.* (2010*a*); N2009, Nutman *et al.* (2009); Hf2010, Hoffmann *et al.* (2010). Apart from the JTA, the ratios and $CaO + Na_2O$ addition at the base of the table are calculated using the averaged values in the table.

[1]JTA major element data are the averaged anhydrous contents of the Newcastle rocks from Hastie *et al.* (2010*a*). JTA trace element averages are from the same paper except for Sr and transition element averages that are in parentheses, which are new published values from Table B2, Appendix B.

[2]TTG averages from Hoffmann *et al.* (2010) include homogeneous TTG analyses from the paper's appendix.

[3]TTG averages from Condie (2005) are obtained by averaging the data from the paper's supplementary data file.

[4]Fe_2O_3 calculated from FeO presented by Drummond *et al.* (1996). It should be noted that the major element data from Drummond are subsequently not re-normalized to 100% after calculating Fe_2O_3.

[5]Fe_2O_3 average from Nutman *et al.* (2009) is derived from samples that do not present combined FeO and Fe_2O_3 values.

[6]MgO value in parentheses is the average MgO content of the JTA if samples AHWG18 and 19 are not included (see text for details).

[7]Cobalt average not included in overall mean value as the number is extremely high.

and high large ion lithophile element (LILE) contents with Sr > 400 ppm (Table 1) (e.g. Defant *et al.*, 1991, 1992; Drummond *et al.*, 1996; Martin, 1999; Condie, 2005; Castillo, 2012). Martin *et al.* (2005) divided adakites into (1) a high-SiO_2 adakite (HSA) subgroup that represents 'type' adakites and (2) a low-SiO_2 adakite (LSA) subgroup that represents high-Mg andesites (Table 1). The HSA have lower MgO (0·5–4 wt %), $Fe_2O_3 + MgO + MnO + TiO_2$ ~7 wt %, $CaO + Na_2O$ contents <11 wt % and La/Yb ≥ 20 (Table 1).

There are several theories published to explain the generation of Cenozoic adakites, such as melting of lower crustal sources and fractional crystallization processes (e.g. Macpherson *et al.*, 2006; Shuto *et al.*, 2013). However, the most widely accepted model for forming Cenozoic adakites is the partial melting of subducting basaltic crust that has been transformed into amphibolite, garnet amphibolite or eclogite (e.g. Kay, 1978; Kepezhinskas *et al.*, 1995; Yogodzinski *et al.*, 1995, 2001; Drummond *et al.*, 1996; Martin, 1999; Rapp *et al.*, 1999; Foley *et al.*, 2002; Martin *et al.*, 2005; Moyen & Stevens, 2006; Moyen, 2009; Ayabe *et al.*, 2012; Sato *et al.*, 2013). Experimental studies and field evidence also suggest that, when ascending adakitic slab melts pass through the mantle wedge, the magma assimilates peridotite, resulting in the hybridization of the slab melt (lower SiO_2 and higher MgO and transition element contents) (e.g. Kepezhinskas *et al.*, 1995; Rapp *et al.*, 1999; Tsuchiya *et al.*, 2005; Sato *et al.*, 2013).

High-SiO_2 adakites (not LSA) are considered to be compositionally similar to mid- to late Archaean (~3·5–2·5 Ga) TTGs [e.g. high Al_2O_3, Na_2O and Sr contents, high La/Yb ratios and low heavy rare earth element (HREE) concentrations] and both show evidence that suggests that they interacted with a mantle wedge (e.g. high MgO and transition element contents) (e.g. Martin & Moyen, 2002; Moyen and Martin 2012; Smithies *et al.*, 2003; Moyen, 2009). Thus, although controversial (e.g. Macpherson *et al.*, 2006; Castillo, 2012), studies of present-day adakites, in addition to experimental petrology and numerical modelling of TTG suites (e.g. Clemens *et al.*, 2006; Laurie & Stevens, 2012), have led to the commonly published proposal that mid- to late Archaean TTGs are formed by partial melting of subducting Archaean oceanic plates (e.g. Smithies *et al.*, 2003; Martin *et al.*, 2005). Nevertheless, it should be noted that generating Archaean TTG magmas has also been explained using non-subduction environments (similar to alternative adakite models). These environments include the partial melting of lower oceanic plateau crust, fusion of thickened mafic crust and/or anatexis of delaminated mafic crust (e.g. Atherton & Petford, 1993; van Thienen *et al.*, 2004; Smithies *et al.*, 2009; Zhang *et al.*, 2013).

In contrast to younger Archaean TTG suites, Eoarchaean TTGs do not have compositions comparable with HSA because they generally have higher SiO_2 and Zr contents and lower TiO_2, Al, Sr, MgO, Ni, Cr and V concentrations (Smithies, 2000; Martin & Moyen, 2002; Smithies *et al.*, 2003; Martin *et al.*, 2005; Nutman *et al.*, 2009) (Table 1). Therefore, how are the Eoarchaean TTG suites generated? Although models to explain the generation of HSA and the younger Archaean TTG suites are controversial, it would be beneficial to discover a modern adakite example that has a composition similar to the Eoarchaean TTG to help us determine if subduction [or subcretion, Bedard *et al.* (2013)] is a viable process on the early Earth.

Newcastle Volcanics (Jamaican-type adakites)—modern analogue of Eoarchaean TTG?

The Newcastle lavas are altered, have quartz, plagioclase and amphibole phenocrysts, and have 64·6–72·2 wt % SiO_2, 14·5–15·9 wt % Al_2O_3, low K_2O of 0·1–1·1 wt % and a high average Na_2O abundance of 5·8 wt % (anhydrous values of 67·9–73·4 wt % SiO_2, 15·1–16·1 wt % Al_2O_3, K_2O of 0·1–1·2 wt % and Na_2O of 5·9 wt %) (Supplementary Data Fig. A5, Appendix A). The lavas have moderately high abundances of LILE and light REE (LREE) (e.g. average La and Th concentrations are 13·87 and 2·89 ppm respectively) and correspondingly low Yb and Y contents of 0·5–0·9 and 5·4–12·8 ppm to give an average La/Yb ratio of ~20 (Table 1). On a normal mid-ocean ridge basalt (N-MORB) normalized multielement diagram the Newcastle samples have negative Nb–Ta anomalies, positive Zr–Hf anomalies and concave-up middle REE (MREE)–HREE patterns (Fig. 2a).

Relative to andesite–dacite–rhyolite (ADR) suites the Newcastle rhyodacites have high Na_2O contents, adakitic-like K_2O/Na_2O (<0·5) and much higher La/Yb ratios (Table 1; Supplementary Data Appendix B). The Newcastle Volcanics are compositionally similar, but not identical, to HSA with their sodic character, high silica, $CaO + Na_2O$ ranging from 5·2 to 10·15, and $Fe_2O_3 + MgO + MnO + TiO_2$ from 3·04 to 5·78 (anhydrous ranges are 5·3–10·6 and 3·1–5·9 respectively). The Newcastle lavas also have adakite- and TTG-like low average Nb/Ta values and high Zr/Sm ratios of 12·2 and 85·7 correspondingly (Foley *et al.*, 2002); although some studies demonstrate a larger range in TTG Nb/Ta ratios (e.g. Bédard, 2006).

The Newcastle rocks are not similar to continental K-adakites (e.g. Wang *et al.*, 2005) or sodic rhyolites (Moyen, 2009) as their K contents and K_2O/Na_2O ratios are too low. However, the Newcastle Volcanics are also not analogues of HSA because they have a very low average Sr content of 129 ppm and they mostly lack the higher MgO and transition element contents of many modern-day adakites (Table 1; Supplementary Data Appendix B) (e.g. Ayabe *et al.*, 2012; Sato *et al.*, 2013). Hastie *et al.* (2010*b*) termed the Newcastle Volcanics Jamaican-type adakites (JTA) not only to highlight their adakitic compositions, but to also emphasize the small chemical differences between JTA and 'true' adakites. We continue to argue for a JTA subgroup here, which can be used alongside the geochemically distinct

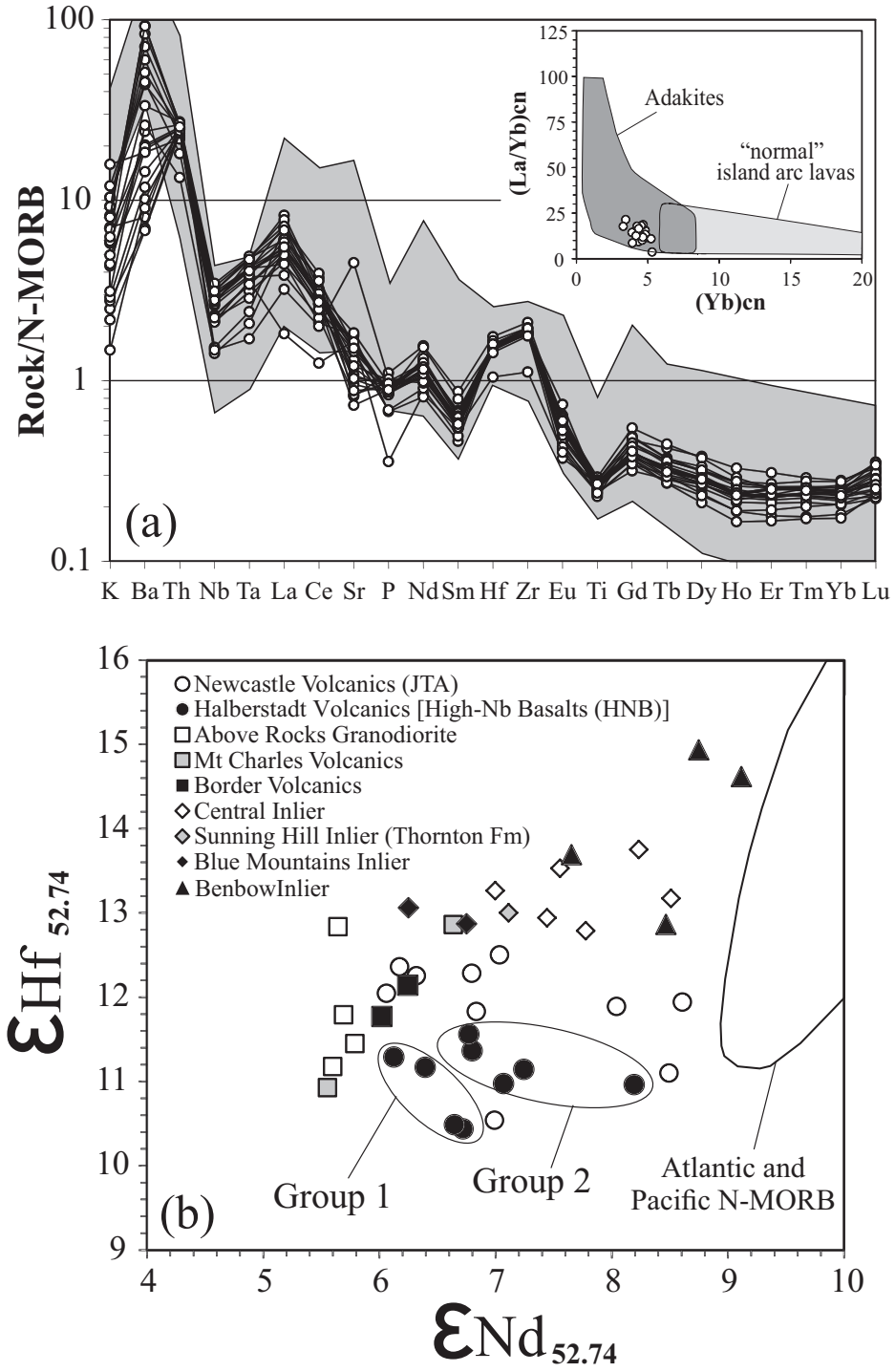

Fig. 2. (a) N-MORB normalized multi-element plot for the Newcastle rocks (Jamaican-type adakites: JTA) with a chondrite-normalized $(La/Yb)_{cn}$–$(Yb)_{cn}$ diagram inset. Grey field on the multi-element plot represents Late Archaean to Cenozoic adakites (see Hastie *et al.*, 2010*a*, for references). Normalizing values are from McDonough & Sun (1995) and Sun & McDonough (1989). (b) $\varepsilon Nd_{52\cdot74}$–$\varepsilon Hf_{52\cdot74}$ plot showing the JTA and Halberstadt lavas relative to the surrounding Jamaican island arc lavas and intrusive rocks from the Central, Blue Mountains, Benbow, Above Rocks and Sunning Hill Cretaceous inliers. (See Fig. 1 for location information and Supplementary Data Table B4 for data and data sources.) Group 1 and 2 refer to subgroups of the Halberstadt Volcanics (see text for discussion).

HSA and LSA of Martin *et al.* (2005). Furthermore, it is striking how similar the JTA average composition is to the average composition of Eoarchaean TTG rocks (Table 1). For many elements (e.g. Ti and Zr) the JTA are more TTG-like than the other adakite compilations. Importantly, the JTA have the low Sr and transition element contents similar to early Archaean TTG suites. Also, the JTA are compositionally similar to

the med-HREE TTG subgroup that has recently been proposed by Moyen & Martin (2012).

DATA AND ANALYTICAL METHODS

The JTA, the Halberstadt Volcanics and island arc rocks from the Cretaceous inliers that surround the Wagwater Basin were analysed for major and trace element and Nd–Hf isotope compositions at Cardiff University, the University of Edinburgh, the NERC Isotope Geosciences Laboratory and the Arthur Holmes Laboratory, Durham University. All the data are given in Supplementary Data Tables B1–B4, Appendix B, along with the analytical methods.

FORMING THE JTA WITH FRACTIONAL CRYSTALLIZATION, MIXING AND ASSIMILATION PROCESSES

Fractional crystallization of Halberstadt magmas to form the JTA

The discovery of JTA-like (Ryozen low Sr/Y) adakites in Japan (Shuto *et al.*, 2013) that can be generated by fractional crystallization processes suggests that the JTA in Jamaica may have also formed by similar processes and not by the fusion of oceanic plateau material. However, in the following sections we use field evidence and several geochemical models to argue that the Jamaican data do not support a fractional crystallization origin for the JTA.

Up to 80–90% fractional crystallization is required to generate TTG-like or adakite-like liquids from a basic melt (e.g. Drummond *et al.*, 1996). Evidence for large accumulations of basic–intermediate plutonic or volcanic rocks that could represent cumulates or parental bodies to TTG liquids are not found in Archaean terranes (e.g. Smithies, 2000; Condie, 2005; Moyen & Martin, 2012). Similar accumulations are also not found near the JTA despite the fact that they are located in an extensional basin (Fig. 1c) (Jackson & Smith, 1978; Jackson *et al.*, 1989).

$^{40}Ar/^{39}Ar$ data indicate that the JTA have an error weighted average age of 52·74 Ma, which is consistent with palaeontological data (Jiang & Robinson, 1987). The only other lavas erupted at this time are the Halberstadt high-Nb basalts (Jackson & Smith, 1978). Consequently, if the JTA are derived from the fractionation of a basic parental liquid, the Halberstadt lavas represent the only viable parental magma. Previously, Hastie *et al.* (2011) have shown that the JTA and the Halberstadt lavas have similar age-corrected Nd and Sr radiogenic isotope ratios, but different age-corrected Hf isotope ratios. Thus, the different Hf-isotope ratios suggested that the JTA cannot be directly generated from the fractionation of a Halberstadt parental liquid. However, new Nd–Hf data in Fig. 2b show that the JTA and Halberstadt Volcanics overlap very slightly and that further studies may well confirm a more extensive isotopic similarity. Therefore, Nd–Hf isotope ratios alone could potentially suggest that the JTA can fractionate from Halberstadt magmas. Nevertheless, major and trace element systematics do not support this assumption.

Figure 3a is a SiO_2–Sr variation diagram that suggests that JTA did not fractionate from a Halberstadt parent liquid because the two rock suites form separate liquid lines of descent (different evolutionary trends seen in numerous other variation diagrams; e.g. REE–SiO_2). In Fig. 3a the JTA have a positive trend implying that a Sr-compatible mineral phase (plagioclase) was not fractionating in any significant amount. Figure 3b is a Dy/Yb–SiO_2 diagram modified from Macpherson *et al.* (2006) that implies that high Dy/Yb ratios in Philippine adakites are formed by the fractionation of a garnet-bearing assemblage from a basic arc parental magma. The JTA do not attain the high Dy/Yb ratios seen in adakitic rocks from the Philippines. Additionally, garnet fractionation would produce a negative correlation between decreasing Y and HREE abundances and increasing SiO_2 content on Harker variation diagrams. Such correlations are seen in adakitic rocks in the Philippines (Macpherson *et al.*, 2006), but not in the JTA (Fig. 3c).

Davidson *et al.* (2007) showed that basic arc lavas that are dominated by amphibole fractionation generate negative trends on a Dy/Yb–SiO_2 plot. Figure 3b shows the trend for amphibole fractionation of basic to silicic island arc lavas in the Lesser Antilles. At the SiO_2 contents typical of the JTA the Lesser Antilles arc magmas would eventually evolve to Dy/Yb ratios much lower than those in the JTA. Therefore, the lack of amphibole cumulates and trace element systematics do not strongly suggest that the derivation of the JTA was the result of extensive amphibole-dominated fractional crystallization from a basic parent arc magma.

Thus, differing liquid lines of descent show that the JTA and the Halberstadt lavas are not related to each other by fractional crystallization processes. Also, there is no evidence for substantial plagioclase and garnet fractionation in the JTA data. However, we will show below that the JTA have undergone relatively limited amphibole fractionation, but not from a basic arc parent.

Mixing and assimilation and fractional crystallization (AFC): an isotope approach

In addition to pure fractional crystallization, the Halberstadt magmas could have assimilated arc crust from the surrounding Cretaceous inliers and subsequently fractionated to form a resultant magma with JTA composition. This theory is tested using the 25 new Nd–Hf isotope analyses reported in this study. All samples are age corrected to 52·74 Ma. Figure 2b shows that several of the Jamaican arc units have variable isotopic compositions and it would be possible to construct mixing trends between a large variety of different

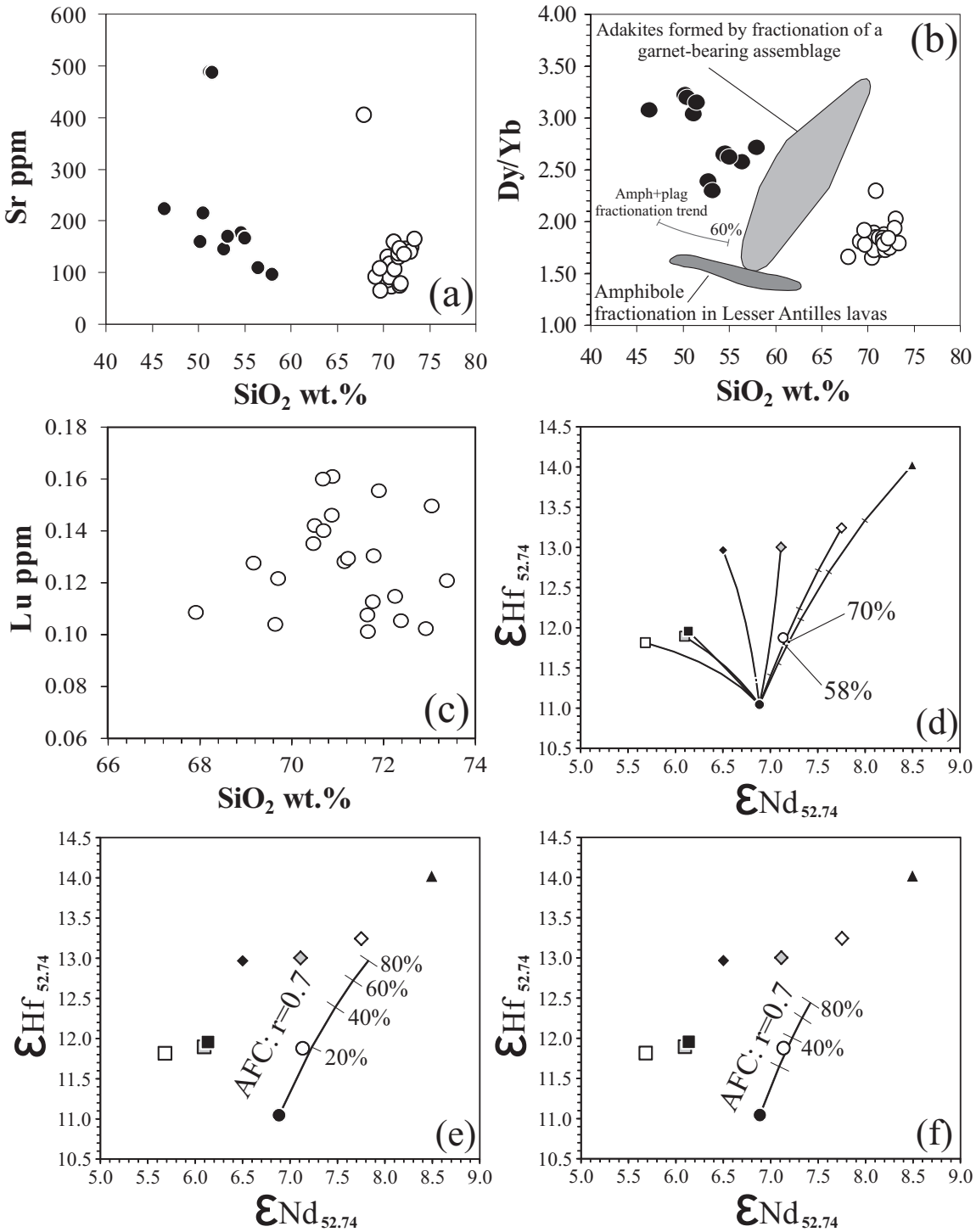

Fig. 3. (a) Sr–SiO_2 variation diagram illustrating the different liquid lines of descent for the JTA and Halberstadt lavas. (b) Dy/Yb–SiO_2 modified from Macpherson *et al.* (2006) and Davidson *et al.* (2007), showing the effects of amphibole and garnet fractionation in generating adakitic rocks. The grey fields represent data trends from the aforementioned papers. (c) Lu–SiO_2 variation diagram. (d) Average $\varepsilon Nd_{52\cdot74}$–$\varepsilon Hf_{52\cdot74}$ compositions for the Jamaican island arc rocks. Mixing trends constructed using equation (1); the tick marks represent 20% intervals. (e, f) Average $\varepsilon Nd_{52\cdot74}$–$\varepsilon Hf_{52\cdot74}$ AFC modelling trends assuming an assimilation/fractionation ratio of 0·7 between Halberstadt lavas and the Benbow and Central Inlier samples, respectively. Sample symbols as in Fig. 2.

samples relative to the Halberstadt rocks. Nonetheless, if a high-temperature alkaline Halberstadt magma were to assimilate substantial proportions of a particular island arc suite, it is likely that it would not simply consume one sample type; it would probably consume a cross-section of the whole suite. Hence, mixing trends have been calculated between the average compositions of the different arc suites and the Halberstadt

lavas in Figure 3d. Simple mixing curves are calculated by

$$\varepsilon C_M = \frac{\varepsilon C_A C_A X + \varepsilon C_B C_B (1 - X)}{C_A X + C_B (1 - X)} \quad (1)$$

where εC_M is the epsilon isotope value of the mixture at 52·74 Ma, εC_A and εC_B are the epsilon isotope ratios in components A and B respectively at 52·74 Ma, C_A and C_B represent the corresponding Hf and Nd concentrations of components A and B respectively, and X is the mass fraction of component A in the mixture (Faure, 1986) (see Supplementary Data Table C1, Appendix C).

The mixing curves between the Halberstadt rocks and the Central Inlier and Benbow Inlier lavas pass close to the JTA. As such, the average $\varepsilon Nd_{(55·74)}$ and $\varepsilon Hf_{(55·74)}$ value of the JTA can be theoretically explained by a mixture of ~58% Halberstadt and ~42% Central Inlier or ~70% Halberstadt and ~30% Benbow Inlier. In addition, using variable assimilation rates isotopic AFC curves can also intersect the JTA average using Halberstadt, Benbow and Central end-members (see Fig. 3e and f for examples). The equations for these calculations are from DePaolo (1981) and include

$$\varepsilon C_l = \frac{\frac{r}{r-1}\frac{C_W}{z}(1 - F^{-z})\varepsilon C_W + C_0 F^{-z} \varepsilon C_0}{\frac{r}{r-1}\frac{C_W}{z}(1 - F^{-z}) + C_0 F^{-z}} \quad (2)$$

$$z = \frac{r + D_0 - 1}{r - 1} \quad (3)$$

where εC_l is the epsilon isotope value of the magma, εC_W is the isotope ratio in the assimilated wall-rock, εC_0 is the epsilon isotope value in the original magma, r is the assimilation/fractionation ratio (set to 0·7 in Fig. 3e and f), F is the fraction of melt remaining, C_0 and C_W represent elemental concentrations in the initial magma and the assimilated wall-rock respectively, and D_0 is the bulk partition coefficient. D_0 is calculated using a standard fractionating assemblage from Woodhead (1988) (5% olivine, 25% clinopyroxene, 60% plagioclase and 10% magnetite) and partition coefficients from McKenzie & O'Nions (1991) and Bédard (2006). To confirm the validity of using the former mineral mode we have performed simple crystallization computations using the MELTS program of Ghiorso & Sack (1995) that suggest that the Woodhead (1988) mode is an excellent approximation. Input parameters and results are given in Supplementary Data Tables C2 and C3, Appendix C.

The composition of the JTA with regard to isotopic composition may be explained by mixing or AFC processes whereby the Halberstadt magmas have consumed part of the Jamaican arc crust represented by the Central or Benbow Inlier lavas. These isotopic findings now need to be tested using trace elements.

Benbow and Central inlier mixing and AFC trends: a trace element approach

Mixing and AFC trends on the $\varepsilon Nd_{(52·74)}$ and $\varepsilon Hf_{(52·74)}$ plot suggest that Halberstadt magmas could assimilate arc material with similar compositions to the igneous rocks in either the Benbow or Central Inlier to generate JTA magmas. To confirm this model, the mixing trends need to be assessed using trace element systematics. Direct trace element mixing is investigated by applying the equation

$$C_m = C_A X + C_B (1 - X) \quad (4)$$

where C_m is the concentration of an element in a mixture, C_A and C_B are the abundances of that element in components A and B respectively, and X is the proportion of component A. For AFC processes it is assumed that primary Halberstadt magmas would fractionate the gabbroic mineral assemblage of Woodhead (1988) as well as assimilating Jamaican arc crust. The trace element AFC processes can be calculated using the following equation from DePaolo (1981):

$$C_l = C_0 \left[F^{-z} + \left(\frac{r}{r-1} \right) \frac{C_W}{z C_0} (1 - F^{-z}) \right] \quad (5)$$

where C_l is the concentration of an element in the resultant magma and other variables are as in equation (2). Input parameters and results are given in Supplementary Data Tables C4–C7, Appendix C.

Figure 4a–h shows representative $\varepsilon Hf_{(55·74)}$–trace element ratio and trace element variation diagrams showing mixing, AFC and fractional crystallization trends between the Halberstadt lavas and samples from the Benbow Inlier (Fig. 4a–d) and the Central Inlier (Fig. 4e–h). It can be clearly seen that none of the modelled trends intersect the JTA data on any of the diagrams. Therefore, although isotope systematics suggest that the JTA can be formed by mixing or AFC processes between Halberstadt magmas and Benbow and Central Inlier contaminants, the trace element and isotope-trace element systematics do not support this view.

Can the Border Volcanic rocks explain the generation of the JTA?

Now that the potential involvement of the Halberstadt rocks in the formation of the JTA has been explored, and discounted, we should point out that some of the JTA have similar radiogenic Nd and Hf isotope ratios to the Border Volcanic samples (Fig. 2b). The silicic Border Volcanics (Fig. 1b) are older than the JTA and cannot represent a viable parental magma *sensu stricto.* However, it is possible that a parental arc magma with a similar composition to the Border Volcanics could fractionate to form the JTA. We now briefly explore this idea. The Border Volcanics are a succession of calc-alkaline and plagioclase- and clinopyroxene-phyric basaltic andesite to andesite lavas. They are of a similar age, and are spatially close to the calc-alkaline and

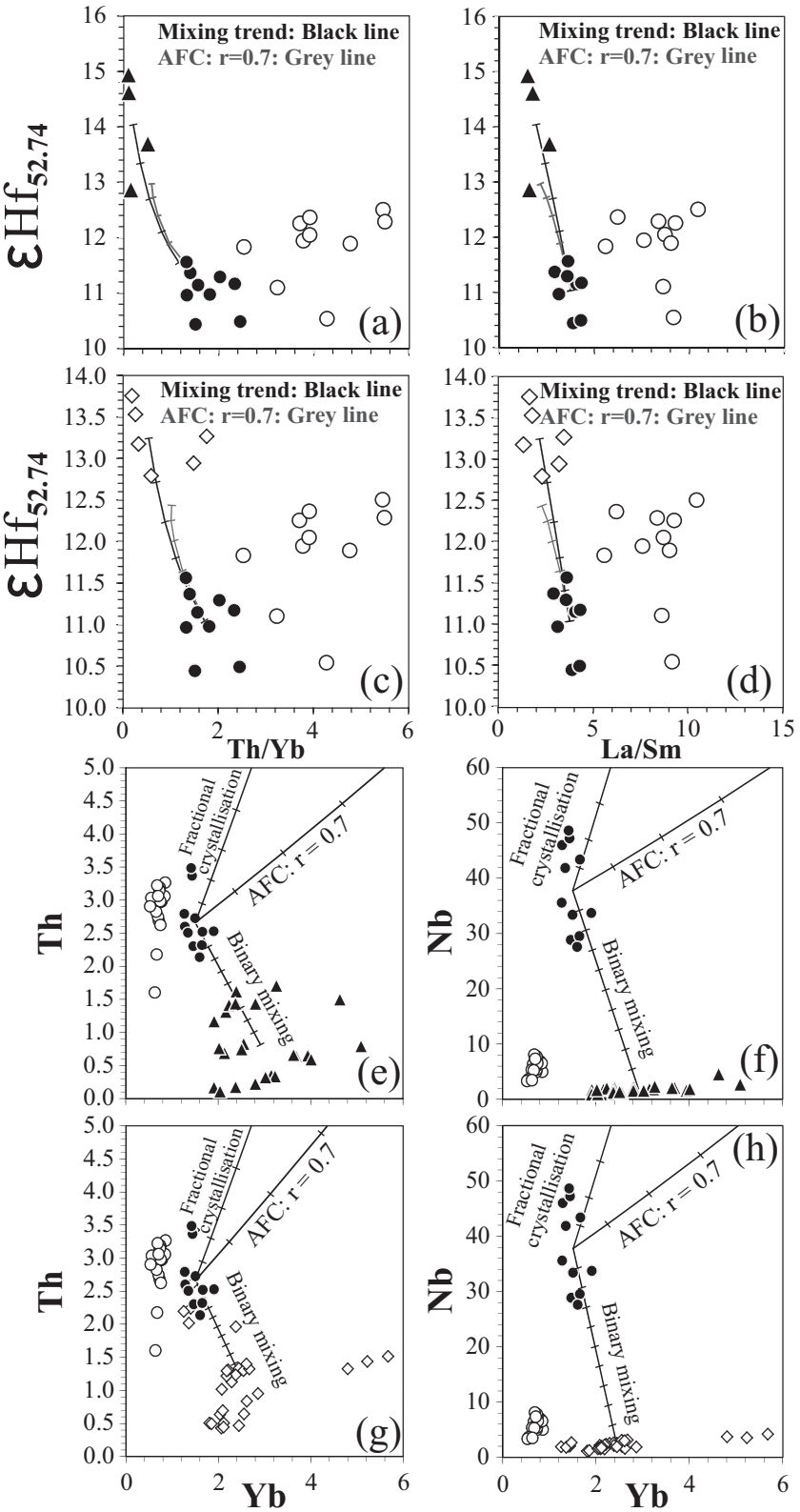

Fig. 4. (a–d) Representative $\varepsilon Hf_{52\cdot74}$ versus trace element ratio diagrams showing mixing and AFC trends between the Halberstadt lavas and samples from the Benbow Inlier (a, b) and the Central Inlier (c, d). (e–h) Representative trace element variation diagrams showing mixing, AFC and fractional crystallization trends between the Halberstadt lavas and samples from the Benbow Inlier (e, f) and the Central Inlier (g, h). Ticks on trends in the $\varepsilon Hf_{52\cdot74}$–trace element ratio diagrams represent 20% intervals (for clarity) of *F* or *X*, whereas in the trace element variation diagrams they represent 10% intervals of *F* or *X*. Sample symbols as in Fig. 2.

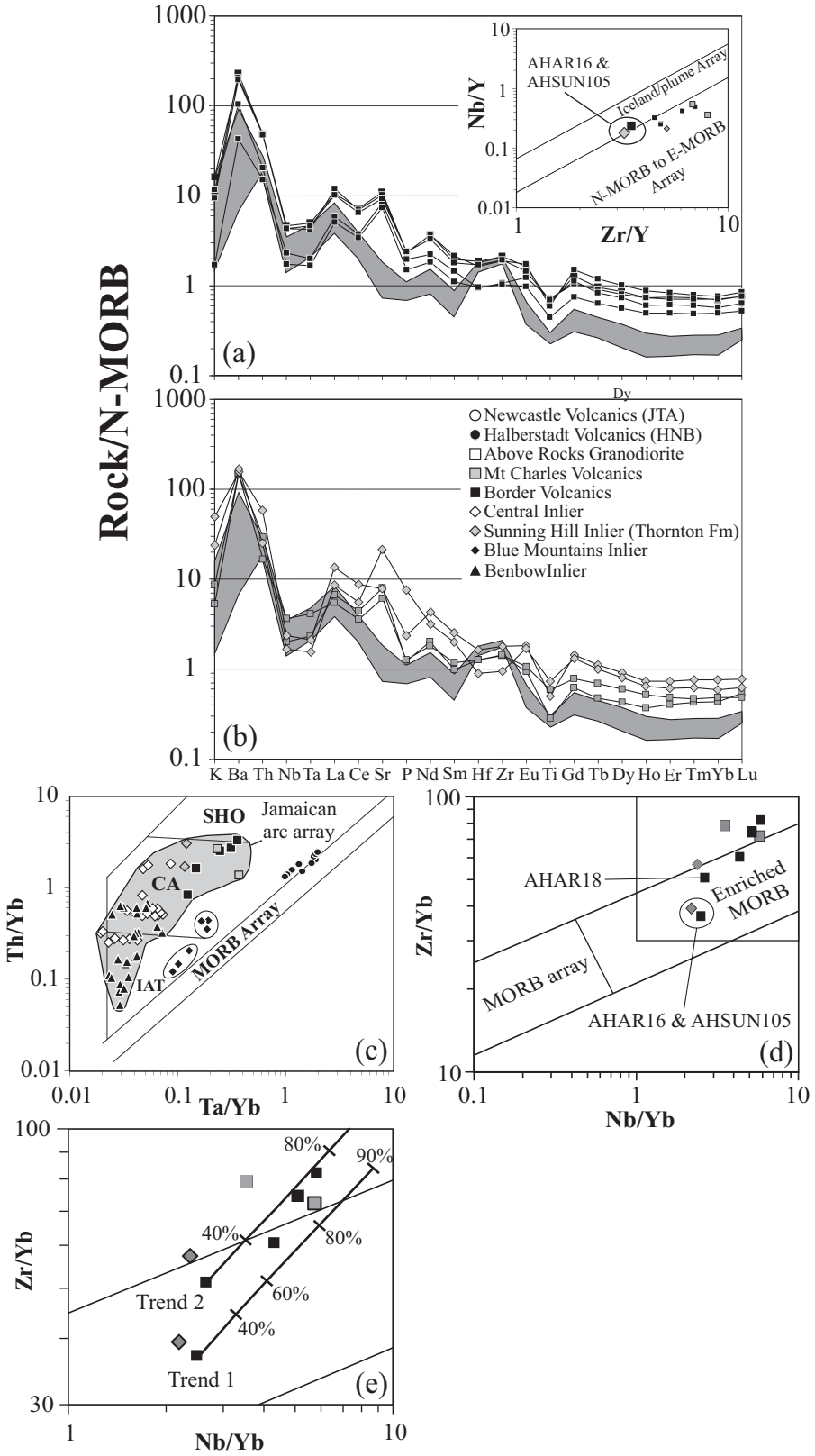

Fig. 5. (a, b) N-MORB-normalized multi-element plots of island arc lavas from the Above Rocks and Sunning Hill inliers. Normalizing values are from Sun & McDonough (1989). Inset Nb/Y–Zr/Y diagram modified from Fitton *et al.* (1997). (c) Th/Yb–Ta/Yb diagram modified from Pearce (1982). IAT, island arc tholeiite; CA, calc-alkaline; SHO, shoshonite fields. (d, e) Zr/Yb–Nb/Yb diagrams of Pearce & Peate (1995). Information about fractional crystallization trends can be found in the text and Trends 1 and 2 are generated using data predominantly from Bacon & Druitt (1988).

quartz- and plagioclase-phyric basaltic andesite to dacitic rocks of the Mt. Charles and Sunning Hill (Thornton Formation) Volcanics (Fig. 1b; Supplementary Data Table B1 and Fig. A2, Appendices A and B). Figure 5a and b shows that all of the lavas have negative Nb–Ta anomalies on N-MORB normalized multielement diagrams and, in the absence of continental crust (e.g. Draper 1986), these anomalies suggest that the rocks are derived from a subduction zone. Figure 5c shows that the lavas have high Th/Yb ratios and plot in the calc-alkaline island arc field above the modified MORB array of Pearce (1982).

The high field strength element (HFSE) and HREE concentrations of the lavas are similar to MORB compositions except for a small Nb–Ta enrichment and MREE–HREE depletion (Fig. 5a). The lavas have negative Ti anomalies and very slight concave-up MREE–HREE patterns (from Gd to Lu) that are commonly attributed to fractionating Fe–Ti oxides and amphibole respectively. Davidson *et al.* (2013) recently presented a Dy/Dy* [chondrite-normalized $Dy/(La^{4/13} \times Yb^{9/13})$] versus Dy/Yb_{cn} diagram to quantify the curvature seen in many chondrite-normalized REE patterns. Amphibole fractionation should generate Dy/Dy* and Dy/Yb_{cn} ratios $<1{\cdot}0$ from a chondritic parent or from a theoretical N-MORB source (e.g. Sun & McDonough, 1989) that has been contaminated with a slab flux. The Border Volcanics have Dy/Dy* from 0·62 to 0·70, but have Dy/Yb_{cn} values >1. Ho/Lu_{cn} from 0·95 to 1·03 may suggest very limited fractional crystallization of amphibole, but the lack of amphibole phenocrysts and high Dy/Yb_{cn} probably rule out extensive amphibole fractionation. The Thornton Formation lavas have similar ratios of Dy/Dy* 0·58–0·71, Dy/Yb_{cn} 1·17–1·35 and Ho/Lu_{cn} ratios from 0·94 to1·04. Mt. Charles Volcanics have Dy/Dy* from 0·49–0·69, Dy/Yb_{cn} values 0·96–1·22 and Ho/Lu_{cn} from 0·69 to 1·07. Therefore, as with other studies on island arc successions (e.g. Woodhead, 1988; Jolly *et al.*, 1998; Davidson *et al.*, 2007) the evolution of these Jamaican basic to silicic arc lavas can be explained by predominantly olivine, plagioclase, clinopyroxene and magnetite fractionation ± a small amount of amphibole.

Samples AHAR16 and AHSUN105 have fairly basic compositions and have not undergone the large degrees of fractionation seen in the other samples (Supplementary Data Table B1, Appendix B). These samples plot on the boundary between Icelandic (mantle plume) basalt and N-MORB on the Nb/Y–Zr/Y diagram of Fitton *et al.* (1997) (inset of Fig. 5a). This, together with elevated Nb concentrations in Fig. 5a, suggests derivation from a more enriched mantle source than the majority of N-MORB. Additionally, these basic lavas plot in the enriched (E)-MORB section of the global MORB array on the Zr/Yb–Nb/Yb diagram of Pearce & Peate (1995) (Fig. 5d). The remaining silicic samples trend towards high Zr/Yb ratios and plot above the MORB array. Similar high Zr/Yb ratios in other basic island arc lavas have been previously explained by the mobilization of Zr from the subducting slab via a partial melt (e.g. Pearce & Peate, 1995; Neill *et al.*, 2010). Therefore, could these arc lavas be slab melts and represent precursors to the JTA? We model the potential fractional crystallization of the Border Volcanics by using a gabbroic modal mineral assemblage from Woodhead (1988) (5% olivine, 25% clinopyroxene, 60% plagioclase and 10% magnetite). The plagioclase modal percentage should probably be a little lower to allow a higher Sr content to be developed in the subsequent melts. For example, fractionating ~50% plagioclase, ~30% clinopyroxene and ~15% magnetite generates similar trends to those for the Woodhead mode, but with higher Sr contents in the magmas. However, mineral modal percentages and distribution coefficients are so variable that it makes identifying the exact fractionating assemblage extremely difficult. As such, we simply use the Woodhead mode here as it represents a close approximation to the probable mineral mode required. The starting compositions are represented by AHAR16 and AHAR18 separately. AHAR18 is another relatively less evolved sample used to bracket all of the potential compositions for the Border, Mt Charles and Sunning Hill Volcanics. Additionally, because of the predominantly andesitic composition of the Jamaican arc lavas, partition coefficients are taken from Fujimaki *et al.* (1984) and Bacon & Druitt (1988), except for magnetite and Nb coefficients, which are from Bédard (2006) and McKenzie & O'Nions (1991) respectively (Supplementary Data Table C8, Appendix C). The equation used for our simple fractional crystallization models is

$$C_l = C_0 F^{(D-1)} \quad (6)$$

where C_l is the concentration in the liquid, C_0 is the initial concentration prior to fractional crystallization, D is the bulk partition coefficient of the fractionating assemblage and F is the proportion of melt remaining.

Fractional crystallization trends (AHAR16 and AHAR18) for the gabbroic mineral assemblage using the stated input parameters are shown in Fig. 5e. The trends extend towards higher Zr/Yb and Nb/Yb ratios and can explain the generation of the more silicic Border Volcanics from a basic magma. This simple model shows that higher Zr/Yb ratios, relative to N-MORB, can be the result of fractional crystallization processes and not a slab melt. Therefore, the Border Volcanics are 'normal' island arc rocks that have been derived from a slab-flux metasomatized enriched MORB mantle wedge and subsequent fractional crystallization of a gabbroic mineral assemblage with the possibility of small amounts of amphibole fractionation in the lower arc crust to generate $Ho/Lu_{cn} < 1{\cdot}0$.

However, can these fractionation models be expanded to explain the generation of the JTA? The most evolved Border Volcanic lava has 61·51 wt % SiO_2 (anhydrous: 62·7 wt %) and is nearly as differentiated as some of the JTA. Therefore, if the JTA are derived from the fractional crystallization of Border Volcanic-like

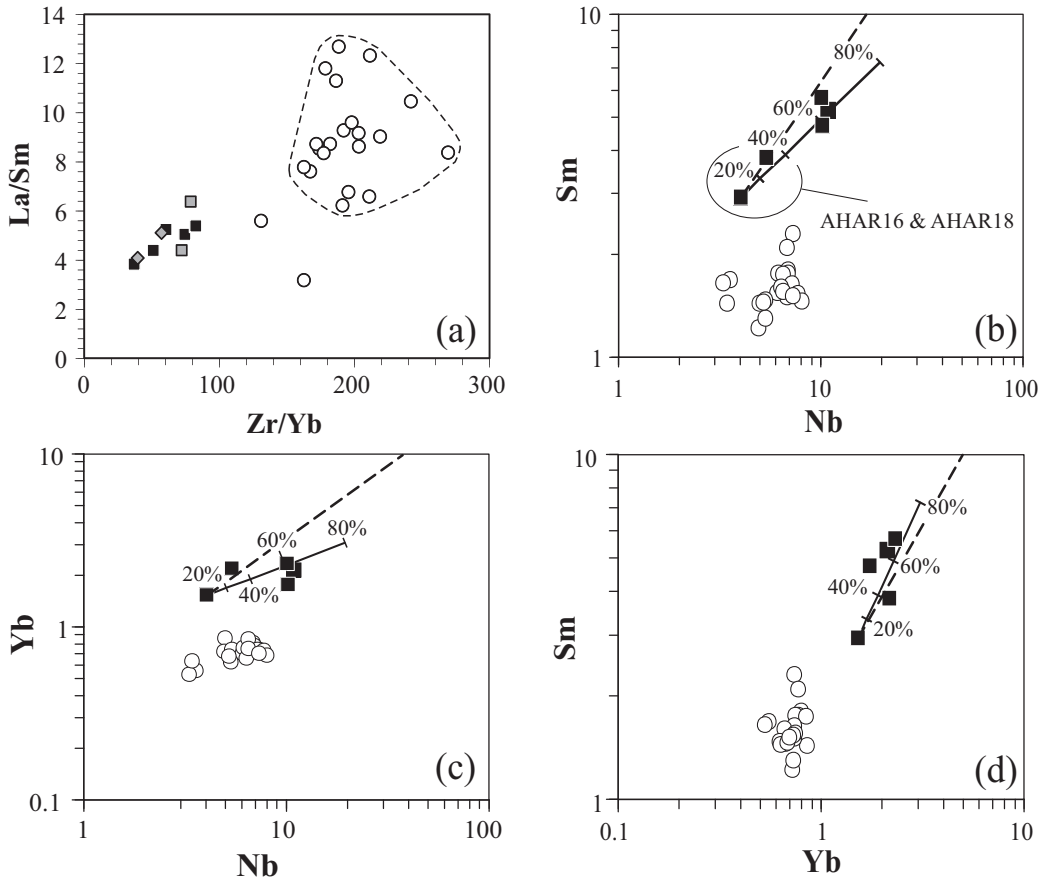

Fig. 6. (a) La/Sm–Zr/Yb diagram showing the dissimilar incompatible ratios for the Above Rocks samples and the JTA. (b–d) Fractional crystallization trends demonstrating that the JTA cannot be derived from a more primitive Border Volcanic sample. Symbols as in Fig. 2. Information about fractional crystallization trends can be found in the text. Trends indicated by a continuous black line are calculated using data from Bacon & Druitt (1988) whereas trends with dashed lines are derived from data predominantly given by Fujimaki *et al.* (1984).

parental magmas it would be expected that the composition of the evolved Border Volcanic lavas would be similar to the JTA composition, but this is not the case. The N-MORB normalized multielement patterns of the Border Volcanic and JTA samples are distinct, with the former having higher concentrations of Sr, P and the MREE–HREE than the latter (Figs 2a and 5a). The differing compositions are highlighted on a La/Sm–Zr/Yb diagram where the 'normal' arc lavas plot in a field separate from the JTA (Fig. 6a).

Fractional crystallization trends using AHAR18 as a starting composition (this sample has the lowest concentration of incompatible elements) are shown in Nb, Sm and Yb variation diagrams in Fig. 6b–d (Supplementary Data Table C8, Appendix C). These trends clearly show that, although the JTA and Border Volcanic lavas have similar radiogenic isotope ratios, the former cannot be formed from the fractional crystallization of a parent magma similar in composition to the Border Volcanic rocks. Even if AHAR16 is used as the starting composition or the fractionating mineral mode is changed to another mineral assemblage (e.g. the low-*P* amphibole assemblage of Macpherson *et al.*, 2006; 74·3% plagioclase, 21·5% amphibole and 4·2% magnetite), the JTA compositions cannot be replicated.

Summary

Major and trace element and trace element-radiogenic isotope systematics show that in contrast to the JTA-like rocks in Japan (Shuto *et al.*, 2013), the Jamaican JTA cannot be modelled with mixing, fractional crystallization or assimilation processes from any viable parental magma on Jamaica.

JTA AND POSSIBLE EOARCHAEAN TTG PETROGENESIS

The JTA source region and modelling parameters

With the previous modelling in mind, we propose that the JTA can be derived only by partial melting of a metabasic source. We explore this option here with updated partial melt models, with an emphasis on varying mineral and melt modes from published high pressure–temperature experiments.

The geochemistry of the JTA [e.g. low Sr contents (<400 ppm), concave-upwards REE patterns, and

average N-MORB normalized (nmn) Gd/Yb ~1·8] requires plagioclase, amphibole and garnet, respectively, to remain stable in the residue [see Hastie *et al.* (2010*b*) for more information]. Such an assemblage will be stable from ~1·0 to 1·6 GPa and will undergo fluid-absent (vapour-absent) partial melting at ~900°C (e.g. Rushmer, 1991; Sen & Dunn, 1994*a*; Wolf & Wyllie, 1994; Patiño Douce & Beard, 1995; López & Castro, 2001; Zhang *et al.*, 2013). Plagioclase is not stable in experiments carried out at these temperatures and pressures under water-saturated conditions (e.g. Peacock *et al.*, 1994).

Several experimental studies on metabasic or intermediate material have documented the phase changes during dehydration of amphibole at the required *P–T* conditions to stabilize a plagioclase- and garnet-bearing amphibolite residue (Sen & Dunn, 1994*a*; Wolf & Wyllie, 1994; Patiño Douce & Beard, 1995; Springer & Seck, 1997). Here we shall investigate these starting amphibolite and garnet amphibolite sources to explain the derivation of the JTA. Our modelling will also investigate compositionally different metabasic sources that include N-MORB, E-MORB, ocean island basalt (OIB) (Sun & McDonough, 1989), average Caribbean Oceanic plateau (COP) (Hastie *et al.*, 2008), and average Ontong Java Plateau (OJP) (Fitton & Godard, 2004; Tejada *et al.*, 2002). Partition coefficients for low-temperature fusion of a metabasic protolith to generate TTG partial melts are taken from Bédard (2006). However, there is a concern related to the widely variable (and controversial) Nb distribution coefficient for amphibole in intermediate to silicic melts (e.g. Ewart & Griffin, 1994; Klein *et al.*, 1997; Hilyard *et al.*, 2000; Martin *et al.*, 2005; Bédard, 2006; Tiepolo *et al.*, 2007; Laurent *et al.*, 2013). Full discussion on the choice of Nb partition coefficient in amphibole is provided in Supplementary Data Appendix C (p. 11 and the caption to Table C9).

Partial melt models

Garnet-free amphibolite

High $(Gd/Yb)_{nmn}$ ratios (JTA average ~1·8) suggest that small amounts of residual garnet remain in the JTA source region, thus requiring the metabasic protolith to be located at a depth of >30 km (>1·0 GPa) (e.g. Martin *et al.*, 2005; Hastie *et al.*, 2010*b*). This is also the case for Eoarchaean TTG suites [e.g. average $(Gd/Yb)_{nmn}$ ~2·2; Nutman *et al.*, 2009]. To test this, a garnet-free amphibolite is modelled to determine if high $(Gd/Yb)_{nmn}$ ratios can be achieved. This is important because garnet-free greenstones and amphibolites are regarded as important constituents of island arc crust and are therefore a potential source for JTA and TTG magmas (e.g. Beard & Lofgren, 1991; Médard *et al.*, 2006; Davidson *et al.*, 2007).

We start by modelling partial melting of an average garnet-free amphibolite based on data from Beard & Lofgren (1991). Those researchers reported subsolidus modes for five arc-derived amphibolites (metamorphosed basalts and andesites) at 3 kbar and 850°C (Beard & Lofgren, 1991, table 5) and here we average the modes to derive a mean starting mineralogy. The melting mode is calculated from the changing average mineral modes after ~19% dehydration partial melting at 900°C and 3 kbar (Beard & Lofgren, 1991, table 3; Supplementary Data Table C9, Appendix C).

Additionally, because Zr and P concentrations are buffered in the JTA (Fig. 7a and b), an estimated 0·01% and 0·165% zircon and apatite, respectively, are added to the mineral starting mode and are presumed to melt modally. These zircon and apatite proportions are chosen so that they account for approximately half to two-thirds of the Zr and P concentrations in an N-MORB, E-MORB and COP protolith. More information on zircon and apatite is given in Supplementary Data Appendix C (p. 11). Residual ilmenite has the potential to buffer Ti contents, but there is no evidence for Ti buffering in the JTA data (Fig. 7c). Therefore, modal volumes of ilmenite are replaced with magnetite in the original mineral and melt modes of Beard & Lofgren (1991). Interestingly, it has been proposed in the literature that fusion of a source region with residual Ti-rich phases (rutile or ilmenite) will generate melts with high Nb/Ta ratios (>25) whereas residual amphibole forms melts with low Nb/Ta (<<25) (e.g. Foley *et al.*, 2002; Hoffmann *et al.*, 2011). Therefore, the low average Nb/Ta ratios of the JTA (~10–16) and Eoarchaean TTG (e.g. ~9: Nutman *et al.*, 2009; ~14: Hoffmann *et al.*, 2011) may suggest amphibole control.

Figure 8 shows N-MORB-normalized multi-element patterns generated by 1–18% partial melting of a shallow metabasic protolith with N-MORB, E-MORB, OIB and COP starting compositions (Supplementary Data Table C9, Appendix C). The non-modal partial melt equation from Shaw (1970) is used for the calculation:

$$C_l = \frac{C_0}{D_0 + F(1 - P)} \quad (7)$$

where C_l is the concentration in the resultant melt, C_0 is the concentration in the source region before partial melting, F is the mass fraction of melt generated, D_0 is the bulk partition coefficient prior to partial melting and P is the average of the partition coefficients weighted by the proportion contributed by each phase to the melt.

None of the garnet-free partial melt models can replicate the low MREE–HREE concentrations of the JTA and the Eoarchaean TTG. Relative to the JTA, the fusion of an N-MORB-like source also produces melts with incompatible element contents that are too low (apart from K, Ce, Nb and Ta), and E-MORB and OIB sources generate melts that are mostly too enriched in LILE and LREE for both JTA and Eoarchaean rocks. A COP source can form melts with incompatible element abundances similar to the JTA and TTG, although the MREE–HREE contents are still too enriched. Additionally, no amount of amphibole fractionation can deplete the MREE–HREE to the concentrations found in the JTA. As an example, Fig. 8 shows

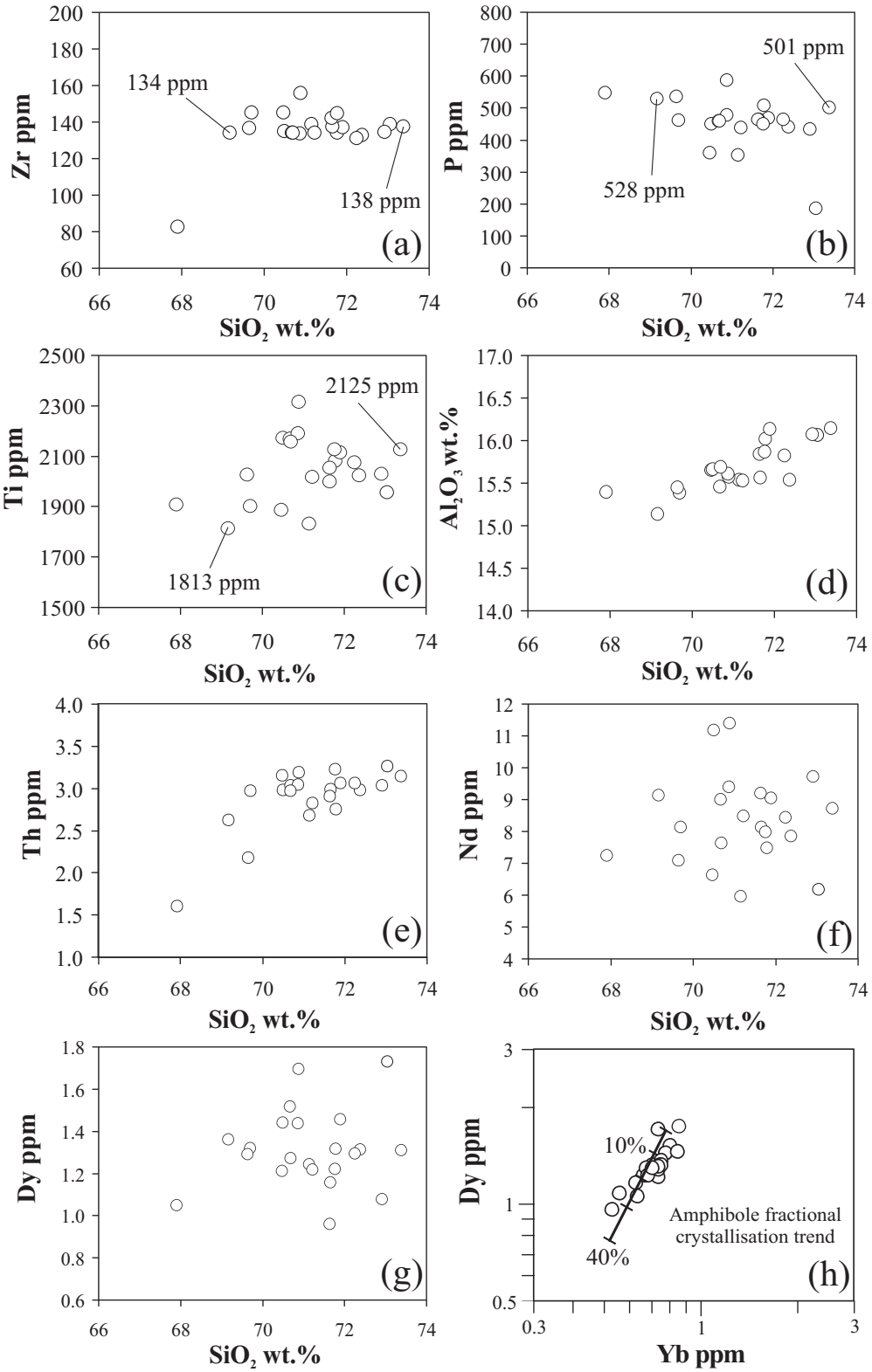

Fig. 7. (a–g) Zr, P, Ti, Al_2O_3, Th, Nd and Dy versus SiO_2 variation diagrams for the JTA. (h) Dy–Yb variation diagram showing a theoretical amphibole fractional crystallization trend from a 10% partial melt derived from data of Sen & Dunn (1994*a*).

the patterns generated by 30% amphibole fractionation of 1% partial melts. Partial melting of garnet-free amphibolite generates $(Gd/Yb)_{nmn}$ ratios from ~0·74 to 1·16 for N-MORB and COP protoliths, which is lower than the JTA average of 1·8 and early TTG average of 2·2 (Nutman *et al.*, 2009) and 2·8 (Hofmann *et al.*, 2011).

Although we have used amphibole as the sole crystallizing phase here, the porphyritic JTA contain quartz,

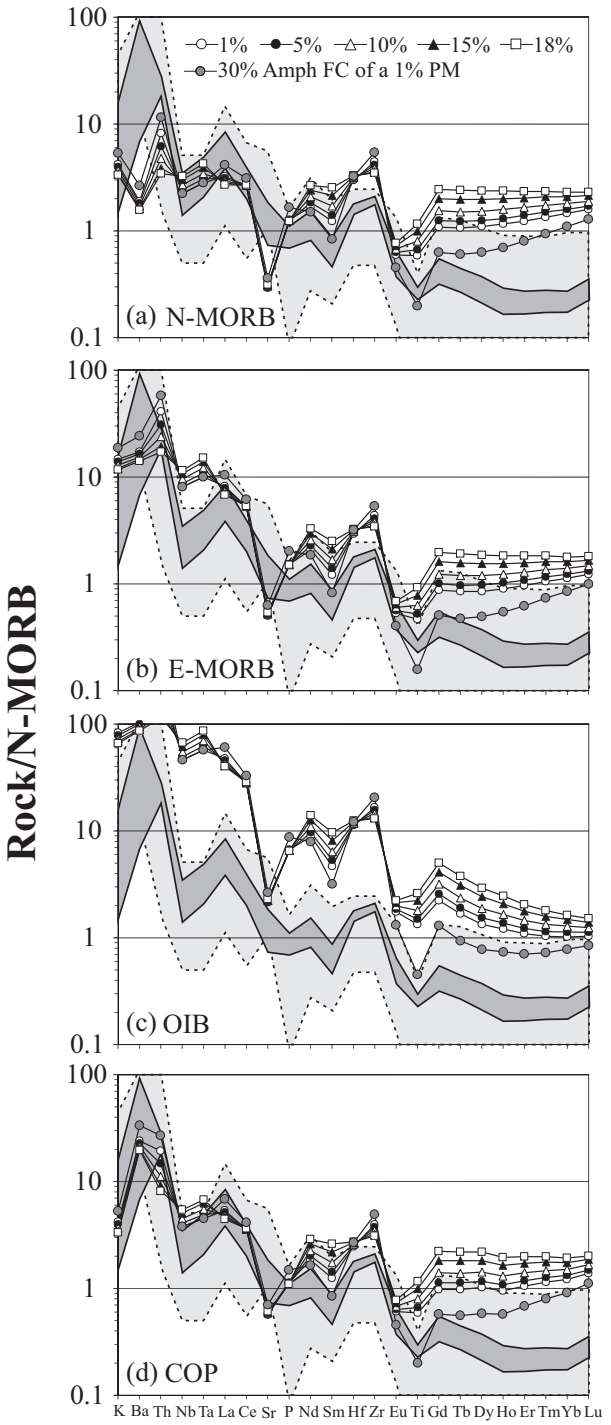

Fig. 8. (a–d) N-MORB normalized multi-element plots of garnet-free amphibolite partial melts based on experimental results from Beard & Lofgren (1991) and N-MORB, E-MORB, OIB and COP as starting compositions. Normalizing values are from Sun & McDonough (1989). Dark and light grey fields represent JTA and Eoarchaean TTG, respectively [TTG data from Nutman *et al.* (2009)]. FC, fractional crystallization; PM, partial melt.

plagioclase and amphibole phenocrysts. Consequently, at least some amount of quartz and plagioclase should have fractionated. Quartz will have D values of zero for all of the investigated trace elements (e.g. Sen & Dunn, 1994*a*), and thus will not be considered further. Plots of Sr and Al_2O_3 vs SiO_2 (Figs 3a and 7d) have positive slopes showing that any proportion of plagioclase in the fractionating assemblage could not have been high because of the high partition coefficient of Sr in plagioclase in equilibrium with a TTG-like melt and the fact that plagioclase is a high-Al_2O_3 phase. Thus, plagioclase is required as a residual phase to buffer the JTA melts at low Sr contents ($<<$400 ppm), but then Sr increases during fractional crystallization because of a lack of plagioclase removal.

Linear trends are not seen on LREE–HREE vs SiO_2 variation diagrams (Fig. 7f and g). This cannot be due to subsolidus silica mobility because of the linear trends with other immobile elements (e.g. Th, Sr and Al_2O_3: Figs 3a and 7d, e) and the LREE–HREE should be immobile during secondary alteration processes. Therefore, the lack of trends consistent with experimental liquid lines of descent on MREE–HREE vs silica variation diagrams cannot be explained by multi-genetic source regions or subsolidus element mobility (Fig. 7f and g). The scattered MREE–HREE data may best be explained by the variable compatibility of MREE–HREE in a fractionating phase (i.e. amphibole; Bédard, 2006).

Consequently, although other phases (e.g. plagioclase, clinopyroxene, apatite and zircon) probably fractionated at depth to some small degree (especially plagioclase), we have no way of knowing the exact proportions of these phases in the crystallizing assemblage because of the absence of cognate xenoliths in the JTA. Thus, we propose that the initial fractionation of the JTA parental magmas at depth was predominantly caused by amphibole. This conclusion is supported by several recent studies presenting geochemical and xenolith evidence for dominant amphibole fractionation in hydrous arc magmas at low to intermediate depths in the crust (e.g. Davidson *et al.*, 2007; Rodríguez *et al.*, 2007; Dessimoz *et al.*, 2012; Rollinson, 2012, 2014).

Garnet amphibolite (with plagioclase)

If a JTA-like lava and an early Archaean TTG-like rock cannot be generated from a garnet-free amphibolite source, can the JTA, including the high $(Gd/Yb)_{nmn}$ ratios in the JTA and Eoarchaean TTG, be explained by fusion of an amphibolite that leaves garnet in the residue? The JTA and early TTG also have low (buffered) Sr concentrations ($<$400 ppm) and low Al_2O_3 contents ($<$19 wt %) that require plagioclase to remain in the residue during dehydration partial melting (Figs 3a and 7d) (e.g. Beard & Lofgren, 1991; Wolf & Wyllie, 1994; Winther, 1996; Martin, 1999; Martin *et al.*, 2005). Plagioclase is not normally stable in metabasic source regions at pressures above ~1·6 GPa (e.g. Winther, 1996; Martin *et al.*, 2005; Clemens *et al.*, 2006; Moyen & Stevens, 2006); therefore, plagioclase-free amphibolites and eclogitic protoliths above ~1·6 GPa are not modelled.

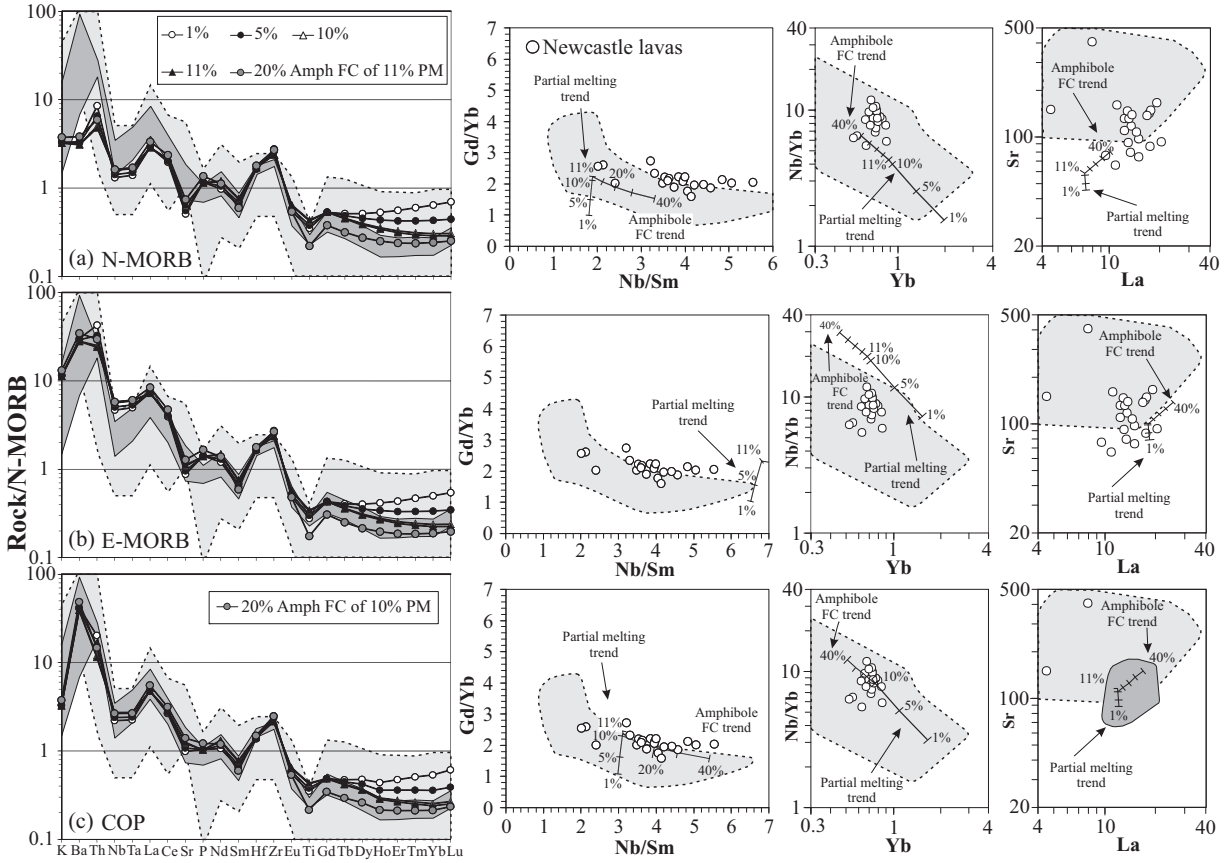

Fig. 9. (a–c) N-MORB normalized multi-element plots, Nb/Sm–Gd/Yb, Nb/Yb–Yb and Sr–La plots showing the results of non-modal partial melting calculations using data of Sen & Dunn (1994*a*). Starting compositions represented by (a) N-MORB, (b) E-MORB and (c) COP. Normalizing values are from Sun & McDonough (1989). Dark and light grey fields represent JTA and Eoarchaean TTG respectively [TTG data from Nutman *et al.* (2009)]. FC, fractional crystallization; PM, partial melt.

Experimental starting mineral modes and melt reactions for partial melting of amphibolite metabasic or intermediate protoliths that leave a residue of amphibole, garnet and plagioclase have been given by Sen & Dunn (1994*a*), Wolf & Wyllie (1994), Patiño Douce & Beard (1995) and Springer & Seck (1997). Our partial melt results using data from these studies generate similar results and, therefore, only those based on Sen & Dunn (1994*a*) are presented here. However, full details and results for the three other studies can be found in Supplementary Data Tables C10–C14, Figs C1–C5, Appendix C.

Results for N-MORB, E-MORB and COP sources are presented in Fig. 9a–c; an OIB source is not shown because it generates melt compositions that are too enriched relative to the JTA and early TTG. Multi-element plots display the full range of trace element concentrations, but Nb/Sm–Gd/Yb, Nb/Yb–Yb and Sr–La diagrams are also included to better illustrate the depletions and enrichments of elements used for the definition of adakites and TTG (e.g. Sr and Yb concentrations).

Sen & Dunn (1994*a*) carried out dehydration melting experiments on an amphibolite that stabilizes garnet and plagioclase in the residue at 1·5 GPa. Partial melt models were constructed using the modal proportions of the starting amphibolite and the melt mode at 1·5 GPa given by Sen & Dunn (1994*a*) (see their p. 406 for the starting mode). The N-MORB partial melt trace element patterns in Fig. 9a do not generally match the whole extent of the MREE–HREE depletion of the JTA, although higher degree melts of E-MORB and COP sources do form JTA-like MREE–HREE patterns. Nonetheless, subsequent fractional crystallization of amphibole from all the model melts can easily produce JTA-like MREE–HREE concentrations for N-MORB, E-MORB and COP starting compositions. The models also replicate Eoarchaean TTG MREE–HREE contents. A Dy–Yb variation diagram (Fig. 7h) shows the importance of dominant amphibole fractional crystallization. The liquid line of descent for amphibole-dominated fractional crystallization explains the JTA data and if plagioclase is included in any large amount (e.g. 60% from Woodhead, 1988) in the fractionating assemblage the good fit between the fractionation trend and the JTA data breaks down. Conversely, smaller proportions of plagioclase do not cause the fit to substantially degrade (approximately up to 15–20%).

Magmas derived from N-MORB and COP protoliths using the data of Sen & Dunn (1994*a*) can have $(Gd/Yb)_{nmn}$ ratios of ~1·8 at ~9–11% partial melting. $(Gd/Yb)_{nmn}$ ratios of ~1·8 can also be achieved if a 10%

partial melt of a COP source undergoes ~8% amphibole fractionation. The LILE and LREE concentrations of the JTA and Ba and Sr contents of Eoarchaean TTG are generally not replicated by fusing an N-MORB starting composition (Sr–La diagram in Fig. 9a). Even subsequent large degrees of amphibole fractionation do not generate JTA or early TTG compositions. Partial melt trends using an E-MORB protolith, with and without amphibole fractionation, form trends that are too enriched relative to the JTA and Eoarchaean TTG (Fig. 9b). However, an ~10% partial melt from a COP source, using data from Sen & Dunn (1994*a*), can generate similar incompatible element concentrations to the JTA and Eoarchaean TTG (Fig. 9c). Moreover, 10–11% partial melting, together with amphibole fractional crystallization, can very closely replicate the whole range of trace element abundances in the JTA.

Consequently, the JTA can be derived by fusing an amphibolite source region with a COP-like composition and residual plagioclase and garnet. In addition, many of the trace element systematics of Eoarchaean continental crust can also be replicated. To further test an oceanic plateau link to the generation of the JTA and the early continental crust, partial melt modelling is repeated in Supplementary Data Fig. C6, Appendix C, using the average trace element composition of the Ontong Java Plateau (OJP) for C_0 values. We thought it sensible to confirm the modelling outcomes by testing another oceanic plateau even though the compositions of oceanic plateau basalts are relatively uniform. As with the COP results, the trace element composition of the JTA and Eoarchaean TTG can be closely replicated using an OJP starting composition.

Adakites are frequently classified based on Sr/Y–Y and chondrite-normalized $(La/Yb)_{cn}$–$(Yb)_{cn}$ systematics (e.g. Martin *et al.*, 2005). Several papers have been dedicated to discussing the variability of these geochemical parameters (e.g. Moyen, 2009) and so we shall not discuss this further. However, Supplementary Data Table C15 and Fig. C7 in Appendix C present the Sr, Y, La and Yb modelling results for the partial fusion of a garnet- and plagioclase-bearing amphibolite COP-like source region with subsequent amphibole fractional crystallization. The results clearly show that these models can explain the Sr/Y–Y and $(La/Yb)_{cn}$–$(Yb)_{cn}$ characteristics of the JTA and Eoarchaean TTG.

Possible island arc protoliths for the JTA and Eoarchaean TTG

The Border Volcanics and some of the JTA have similar Nd–Hf age-corrected radiogenic isotope ratios (Fig. 2b), which suggests that the Border Volcanics lavas could also undergo partial melting to form the JTA. Figure 10a–c shows that melts formed from a garnet amphibolite with the composition of the Border Volcanics have enriched incompatible element patterns that are not similar to the JTA (Supplementary Data Table C16, Appendix C). In addition, small outcrops of latest Cretaceous metamorphic rocks occur in the Blue Mountains Inlier, eastern Jamaica, and include blueschists and greenschists of the Mount Hibernia Schists and amphibolites of the Wesphalia Schists (Draper, 1986; Abbott *et al.*, 1996; Abbott & Bandy, 2008; West *et al.*, 2014) (Fig. 1b and Supplementary Data Fig. A4, Appendix A). The Mount Hibernia Schists are dominated by metabasic igneous rocks, and recently West *et al.* (2014) showed that they are compositionally similar to obducted oceanic plateau rocks found in Jamaica (the Bath–Dunrobin Volcanics: Supplementary Data Fig. A4, Appendix A).The Westphalia Schists were originally thought to include sedimentary, pyroclastic and volcaniclastic components, but the effects of intense metamorphism make identifying pre-metamorphic rock types very difficult (Draper, 1986; West *et al.*, 2014). However, West *et al.* (2014) reported the presence of very limited exposures of metabasic garnet-bearing amphibolites that have island arc-like compositions. If we take the only available analysis of a Westphalia garnet amphibolite [sample 09-1 A of West *et al.* (2014)] as representative of a source composition and use the same modelling parameters as in Fig. 10a–c, the resultant melts are too enriched in incompatible elements to account for the JTA (Fig. 10d–f).

Adam *et al.* (2012) and Nagel *et al.* (2012) have suggested that Archaean TTGs can be derived from the partial melting of island arc-like metabasic protoliths. We test this hypothesis by carrying out partial melt calculations using average Eoarchaean island arc-like metabasalt and boninitic metabasalt compositions from Nutman *et al.* (2009). The compilation of data is largely from Nutman's previous papers and Polat & Hofmann (2003). The results (Fig. 11a–f; Supplementary Data Fig. C8 and Table C17, Appendix C) show that a boninitic source (Fig. 11a–c) generally forms melts that are too depleted in the most incompatible elements relative to Eoarchaean TTGs. In contrast, melts derived from an average Eoarchaean island arc-like metabasaltic source generate melts compositionally similar to Eoarchaean TTG suites.

Some researchers consider Archaean metabasalts to gain their arc-like compositions from crustal contamination processes and not from an Archaean subduction environment. Regardless of the subduction versus non-subduction nature of these rocks the models presented here (and in other papers; e.g. Bédard, 2006) show that Archaean metabasalts can potentially undergo partial melting to generate TTG compositions. However, it is unknown whether the relatively small volumes of Eoarchaean island arc-like metabasic material (e.g. Nutman *et al.*, 2009) could have been the source for the large volumes of Eoarchaean plutonic TTG rocks via intracrustal partial melting.

Summary

The JTA and Eoarchaean TTG could have been derived from the partial melting of metamorphosed oceanic

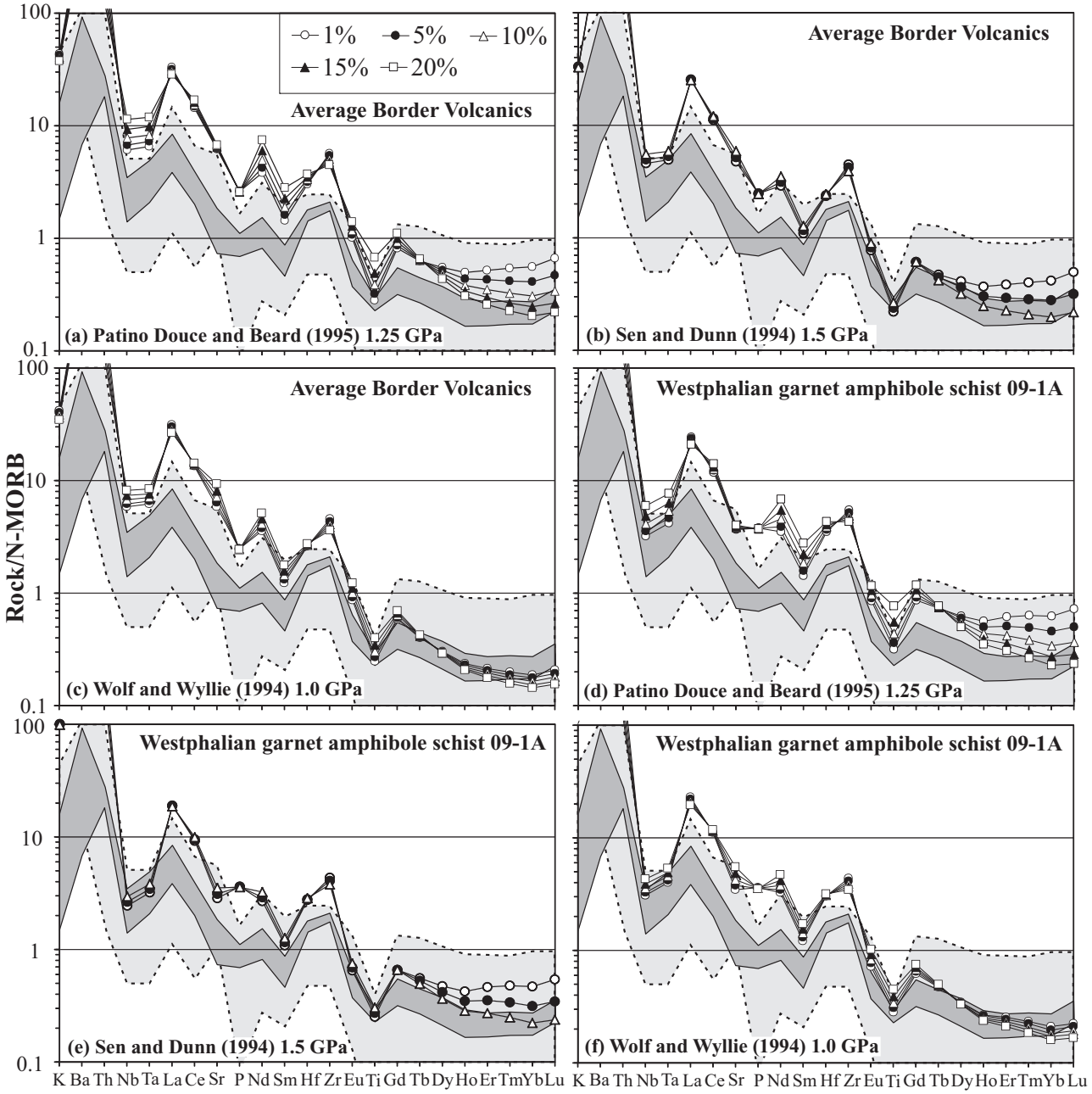

Fig. 10. (a–f) N-MORB normalized multi-element diagrams showing the results of non-modal partial melting calculations using data from Sen & Dunn (1994*a*), Wolf & Wyllie (1994) and Patiño Douce & Beard (1995). Starting compositions are represented by the average Border Volcanic samples (Supplementary Data Table C16, Appendix C) and Westphalia Schist garnet amphibolite sample 09-1A from West *et al.* (2014). Normalizing values are from Sun & McDonough (1989). Dark and light grey fields represent JTA and Eoarchaean TTG, respectively [TTG data from Nutman *et al.* (2009)].

plateau-like metabasic protoliths that leave a residue of amphibole, garnet and plagioclase (and apatite and zircon for the JTA). Partial melt models for melting the base of an oceanic plateau have also been computed by Bédard (2006) and Zhang *et al.* (2013). Their results are very similar to our findings and help support the idea of generating Archaean TTG from oceanic plateau-like source regions, whether this be in a subducting (or subcreting) environment or not.

HALBERSTADT (HIGH-Nb) BASALT GENESIS AND EOARCHAEAN MAFIC ARC ROCKS

The Halberstadt Volcanics

To construct a realistic tectonic model for the generation of the JTA we cannot ignore the petrogenesis of the small succession of Halberstadt high-Nb basalts (HNB) that are of the same age as the JTA (Supplementary Data Fig. A1, Appendix A). We have previously discounted a direct petrogenetic link

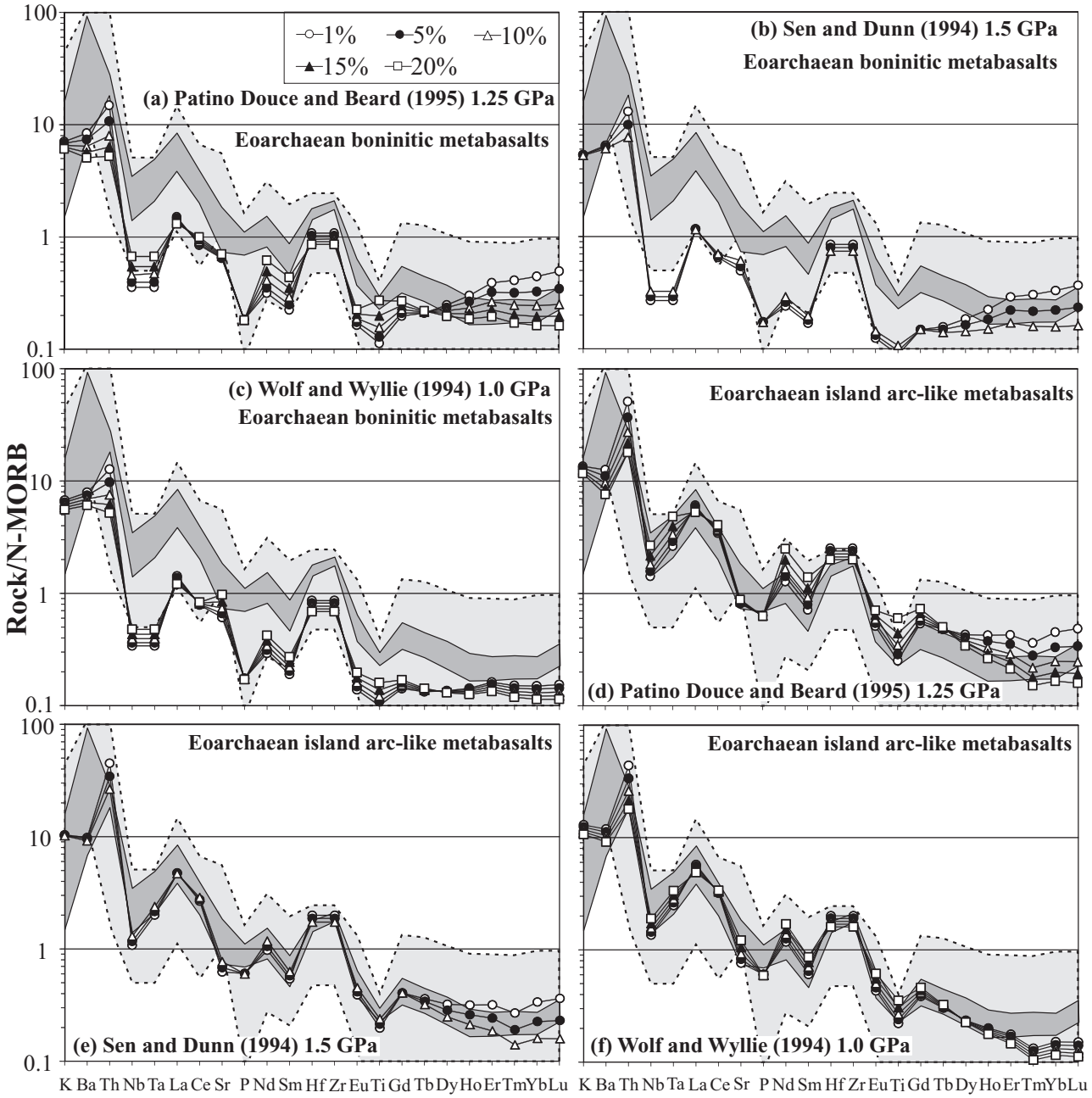

Fig. 11. (a–f) N-MORB normalized multi-element diagrams showing the results of non-modal partial melting calculations using data from Sen & Dunn (1994*a*), Wolf & Wyllie (1994) and Patiño Douce & Beard (1995). Starting compositions are represented by the average trace element compositions of Eoarchaean (>3850–3700 Ma) metamorphosed boninitic and basaltic island arc-like rocks from Nutman *et al.* (2009).

between the HNB and the generation of the JTA, but we now explore the petrogenesis of the HNB so that they can also be integrated into a holistic tectonic model. This may also help us to develop a better tectonic model for Eoarchaean melt generation environments.

High-Nb basalts, with >20 ppm Nb, are associated with adakites in subduction environments, but their petrogenesis is controversial (e.g. Reagan & Gill, 1989; Defant *et al.*, 1992; Kepezhinskas *et al.*, 1995; Sajona *et al.*, 1996; Wyman *et al.*, 2000; Castillo, 2008). The two main hypotheses for their derivation are (1) partial melting of upper mantle that is composed of enriched OIB-like and depleted MORB-like components (e.g. Reagan & Gill, 1989; Castillo, 2008), and (2) partial melting of upper mantle peridotite that has been metasomatized with slab melt components (e.g. Defant *et al.*, 1992; Kepezhinskas *et al.*, 1995, 1996).

The Halberstadt rocks are classified as HNB (Hastie *et al.*, 2011) and form two distinct subgroups with Group 1 lavas having higher LILE, LREE and HFSE abundances and slightly lower HREE contents than Group 2 lavas (Fig. 12a). Group 1 and 2 lavas have different

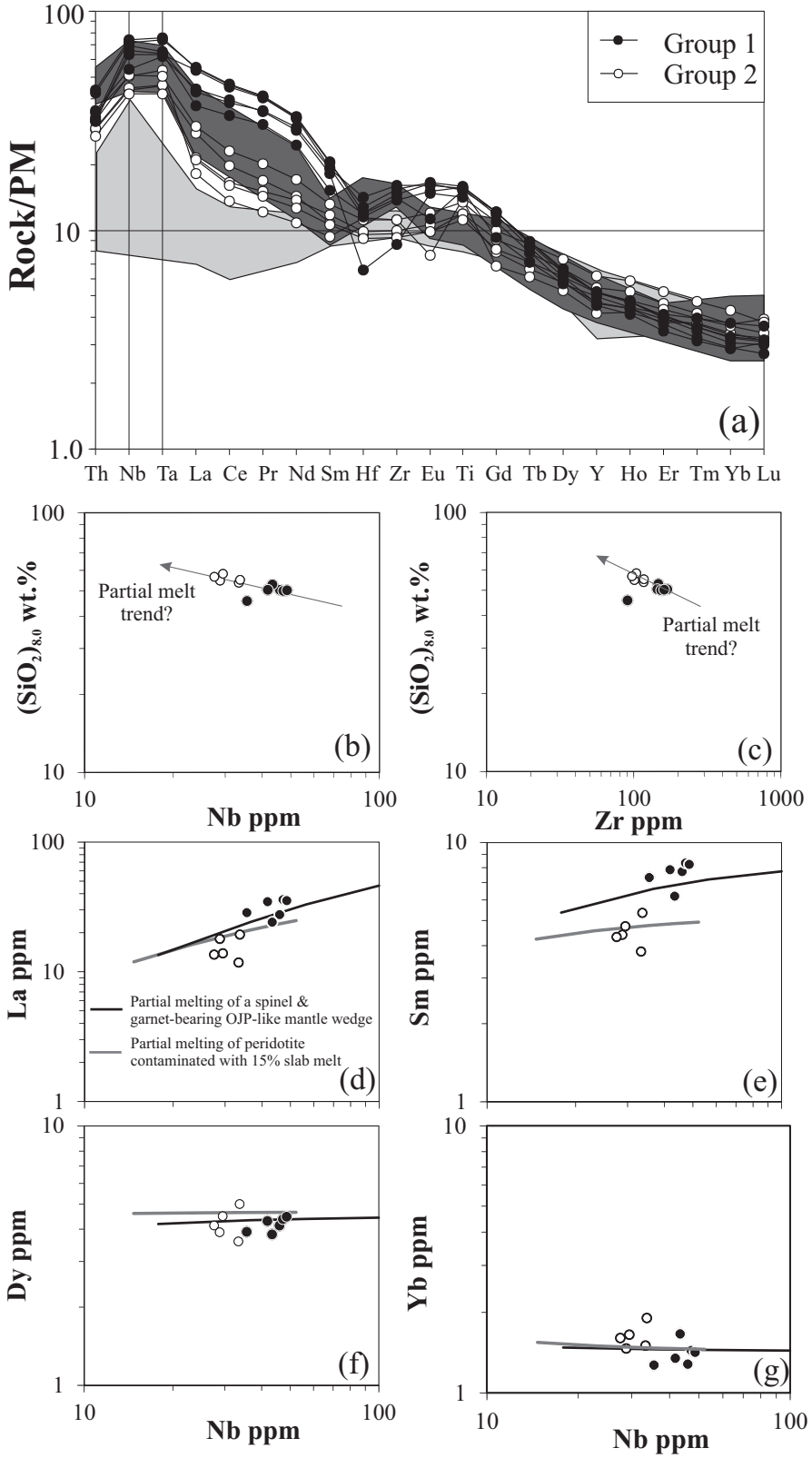

Fig. 12. (a) Primitive mantle (PM) normalized multi-element plot showing Group 1 and 2 Halberstadt lavas. Normalizing values are from McDonough & Sun (1995). Dark and light grey fields represent HNB and Nb-enriched basalt (NEB) respectively (see Hastie *et al.*, 2011, for data sources). (b, c) $(SiO_2)_{8\cdot0}$–Nb and Zr plots [$(SiO_2)_{8\cdot0}$: fractionation correction using $SiO_2 + 0{\cdot}31MgO - 2{\cdot}48$ (Klein & Langmuir, 1989)]. (d–g) Representative incompatible element variation diagrams with various partial melt trends (see text for details).

$\varepsilon Nd_{(55\cdot74)}$ values, which indicates that they are derived from compositionally distinct source regions (Fig. 2b). The Halberstadt rocks also form negative trends on Nb and Zr vs $(SiO_2)_{8\cdot0}$ diagrams that are commonly explained in terms of different degrees of partial melting (Fig. 12b and c). Therefore, the petrogenesis of Groups 1 and 2 has been interpreted as reflecting derivation from isotopically distinct sources undergoing variably small degrees of fusion.

Hastie *et al.* (2011) argued for the Halberstadt lavas to be derived from a mantle source metasomatized by slab melts partly because most of the upper mantle beneath, and adjacent to, Jamaica at ~55 Ma should have been composed of depleted material formed by the generation of the ~90 Ma COP by 20–30% partial melting (e.g. Hauff *et al.*, 1997; Révillon *et al.*, 2000; Kerr *et al.*, 2002*a*, 2002*b*; Hastie & Kerr 2010). However, new data of Neill *et al.* (2011) and Hastie *et al.* (2013) show that undepleted oceanic plateau mantle sources were present below Jamaica in the Tertiary and these sources could have given rise to the Halberstadt lavas.

Figure 13a–c shows small-degree partial melting trends for spinel- and garnet-peridotite source regions with oceanic plateau-like mantle starting compositions (Supplementary Data Table C18, Appendix C). There is a lack of data to determine confidently the composition of the COP mantle source region at this time; thus, data for the OJP are used to determine the composition of the theoretical oceanic plateau source. HNB samples plot between the spinel and garnet trends suggesting that the HNB lavas could be formed from the partial melting of a mantle source that extends across the garnet–spinel transition. Gurenko & Chaussidon (1995) presented mineral and melt modes for a garnet- and spinel-bearing primitive mantle lherzolite. A partial melt model (not shown) suggests that the original mineral proportion of Gurenko & Chaussidon (1995) with 6% garnet generates a trend that cannot explain the derivation of the HNB data. Therefore the original starting mineralogy of Gurenko & Chaussidon (1995) was modified slightly to reduce the garnet modal abundance from 6 to 4%. The modified source region with 4% garnet generates a partial melt trend that passes through the HNB data (Fig. 13a). Primitive mantle-normalized multielement diagrams confirm that Group 1 Halberstadt lavas can be explained by ~0·5–1·0% fusion of a spinel- and garnet-bearing OJP-like peridotite source region (Fig. 13b–d; Supplementary Data Table C19, Appendix C).

Figure 13a also suggests that Group 2 lavas can be explained by slightly larger degrees of partial melting (1·0–2·5%). However, the modelled partial melts cannot replicate the Group 2 LREE–MREE depletion (Fig. 13d). Group 2 samples have an average $(Ce/Ce^*)_{Nd}$ of 0·9, which may suggest a source region contaminated with a slab-derived sedimentary component (e.g. Plank & Langmuir, 1998). Thus, our data suggest that there is evidence for JTA slab–melt interaction in the petrogenesis of the Group 2 lavas.

Slab melt–peridotite interaction?

Experiments show that partial melting of a basaltic source commonly generates silicic melts with low MgO concentrations (e.g. <1·4 wt %: Rapp *et al.*, 1999). Carroll & Wyllie (1989) and Rapp *et al.* (1999) showed that if these silicic melts react with peridotite the resultant liquids will have much higher MgO contents (e.g. 2·4–3·9 wt %: Rapp *et al.*, 1999). Most of the JTA have low MgO contents and only two samples have MgO > 2·0 wt % (AHWG18 and AHWG19). Therefore, the JTA magmas may not have substantially interacted with a peridotite source after anatexis. However, the models we present suggest that ~10–30% amphibole fractionation is required to generate many (but not all) of the JTA. This being so, can amphibole fractionation obliterate a mantle signature?

We model the effects of separating an amphibole-dominated cumulate assemblage from the JTA parental magmas by taking several published analyses of amphibole-rich xenoliths and then estimating the MgO content of the JTA parental magmas by mass balance:

$$C_0 = C_{JTA}(1 - X) + C_C F. \quad (8)$$

This equation is similar to equation (4), but here X is the proportion of solid cumulate material removed, C_{JTA} is the average composition of the JTA lavas and C_C is the composition of the cumulate. Recent studies have reported whole-rock compositions for amphibole-rich lower arc cumulate xenoliths (Rodríguez *et al.*, 2007; Dessimoz *et al.*, 2012). Using compositions from these studies shows that correcting the average JTA composition for the removal of 25% by mass of a typical cumulate generates JTA parental melts with silicic compositions and MgO contents of ~4·1–4·3 wt % (Supplementary Data Table C20, Appendix C).

The Nb/Sm–Gd/Yb diagram in Fig. 9c can be used to estimate the degree of amphibole fractional crystallization for each JTA lava, and these values are used in equation (8) to calculate the original magma compositions of each of the JTA rocks (Supplementary Data Table C21, Appendix C). Some of the JTA (e.g. AHWG14 and AHWG22) have a composition that can be explained without the need for extensive amphibole fractionation. These samples have low calculated parental MgO (<2·0 wt %) and have probably not interacted with a mantle wedge. Also, studies show that silicic (on the dacite–rhyolite boundary) experimental melts derived from basaltic sources can have MgO abundances up to ~3 wt % (e.g. Wolf & Wyllie, 1994; Martin *et al.*, 2005). Thus, even if mass balance implies that a JTA magma had 2–3 wt % MgO these magmas may still be derived from a metabasic source region and ascend without reacting with a mantle wedge. However, some theoretically calculated parental JTA magmas have >3 wt % MgO, which strongly indicates that some of them may have variably interacted with a mantle wedge, and it is possible that the Group 2 lavas are derived from a source contaminated by slab melts.

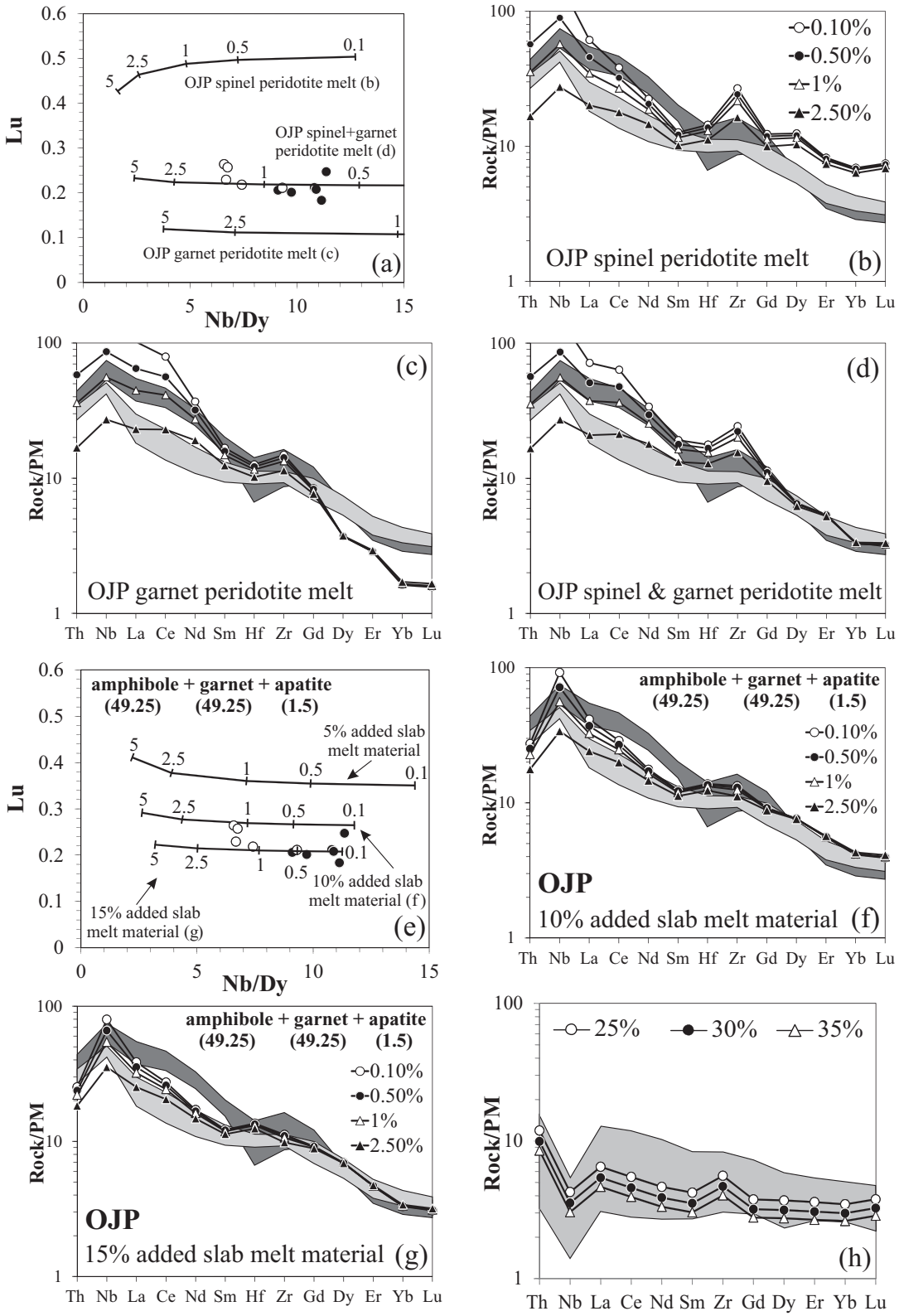

Fig. 13. (a–d) Nb/Dy–Lu plot and primitive mantle normalized trace element patterns linked to (a) that show a range of anhydrous mantle partial melt trends to determine the petrogenesis of the Halberstadt HNB. (e–g) Nb/Dy–Lu plot and primitive mantle normalized diagrams linked to (e) that show a range of hydrous partial melt trends to determine the petrogenesis of the Halberstadt HNB. Dark and light grey fields represent Group 1 and Group 2 HNB, respectively. (h) Primitive mantle normalized diagram showing the results of 25–35% hydrous modal batch partial melting of an OJP source region contaminated with 5% Eoarchaean TTG. The composition of the OJP source region and the average TTG contaminant are from Fitton & Godard (2004) and Nutman *et al.* (2009) respectively. The grey field represents Eoarchaean island arc basalt samples from Nutman *et al.* (2009) (minus sample JG03/03). Normalizing values are from McDonough & Sun (1995).

Magma from a mantle source contaminated with a slab melt

A silicic slab-derived melt ascending through a mantle wedge will fractionate and react with the mantle, thereby converting the peridotite mineralogy to an assemblage of Nb- and Ti-enriched amphibole (pargasite), garnet, phlogopite, clinopyroxene, orthopyroxene and plagioclase (e.g. Carroll & Wyllie, 1989; Johnston & Wyllie, 1989; Sen & Dunn, 1994*b*; Kepezhinskas *et al.*, 1995; Rapp *et al.*, 1999; Prouteau *et al.*, 2001; Tsuchiya *et al.*, 2005). Modelling this interaction is extremely difficult because the petrological processes involved in the multi-stage and polybaric reactions are complex and not fully understood (e.g. Johnston & Wyllie, 1989; Moyen, 2009; Ayabe *et al.*, 2012; Rollinson, 2014). Thus, the model we now present is a simplified version of what in reality must be a highly complex system. The modelling procedure is detailed in Supplementary Data Appendix C (p. 44).

To derive JTA magmas from a subducting slab and have them ascend to interact with the overlying mantle wedge, a pressure range of 1·0–1·6 GPa is required to stabilize residual amphibole, garnet and plagioclase in the downgoing slab. Phlogopite is usually stable at higher pressures (and lower temperatures) in peridotite reaction zones (e.g. Adam *et al.*, 1993; Kepezhinskas *et al.*, 1995; LaTourrette *et al.*, 1995) and a mantle wedge will already contain ortho- and clinopyroxene, so these minerals will not be considered further. We therefore consider a situation in which primary JTA magmas ascend and metasomatize an overlying mantle wedge at pressures $<$1·6 GPa where they precipitate amphibole and garnet. Garnet is stable at low pressures during slab melt–peridotite reactions (e.g. Carroll & Wyllie, 1989; Sen & Dunn, 1994*b*). The JTA magmas are also considered to be saturated in P and Zr so apatite and zircon may also fractionate from the JTA magma in a reaction zone.

The JTA can be largely explained by amphibole fractionation after melt generation; therefore, if we now propose that all of the JTA magmas have fractionally crystallized a garnet and amphibole assemblage the conclusions of the previous JTA petrogenesis models are not valid. However, only the initial JTA magmas would metasomatize the overlying thin mantle wedge. This would armour melt pathways into the Jamaican crust whereby subsequent JTA magmas will predominantly crystallize amphibole (e.g. Tsuchiya *et al.*, 2005; Moyen, 2009). It is also possible that less garnet is required in the JTA crystallizing assemblage if amphibole in the HNB source melts incongruently and forms residual garnet (e.g. Francis & Ludden, 1995). Furthermore, geochemical models (explained in further detail below) involving much higher proportions of amphibole relative to garnet can easily generate Group 2-like compositions; thus, a dominant garnet component is not necessarily required. Large volumes of apatite and zircon could not crystallize from most of the JTA as this would result in negative *P* anomalies and extreme HREE depletion (e.g. Rollinson, 2012). However, if small volumes of apatite and zircon crystallize from the ascending JTA melts, the fractional crystallization trends for the Sen & Dunn (1994*a*) COP data in Fig. 9 are not substantially changed.

In the proposed model, a 10% melt derived from the melting models using the parameters from Sen & Dunn (1994*a*) is fractionated. The modal assemblage that fractionates is composed of amphibole, garnet, apatite and zircon in the proportions 49·245:49·245:1·5:0·01 respectively. The mantle wedge is considered to be a spinel peridotite with a chemical composition required to generate the OJP (see Supplementary Data Table C18, Appendix C). The trace element chemical composition of the peridotite is modified by addition of the average concentration of a trace element in the accumulated crystal extract from the 10% theoretical melt. Subsequently 5–15% of the modal mineralogy of the spinel peridotite is replaced with the amphibole-, garnet- and apatite-bearing mineral assemblage in the proportions 49·25:49·25:1·5. Zircon is considered to be exhausted by $<$0·1% partial melting and is, thus, not included in the peridotite melting assemblage. This crudely simulates the metasomatic replacement of peridotite minerals in the reaction zone and the addition of a slab melt component (Supplementary Data Tables C22–C24, Appendix C). Figure 13e–g shows partial melt trends for a metasomatized OJP-like mantle wedge source region.

Partial melt trends for 10–15% replacement intersect the majority of the HNB data, but primitive mantle-normalized multi-element diagrams show that only the Group 2 depleted LREE–MREE compositions can be replicated. Therefore, the models suggest that the Group 2 rocks are derived from ~1·0–2·5% partial melting of a slab-metasomatized mantle wedge source region. This may explain why Group 2 lavas slightly overlap the JTA field on an εNd–εHf diagram (Fig. 2b), but the Group 1 lavas do not. Figure 13e–g shows the results for ~50:50 amphibole and garnet, but similar results can be obtained by changing this ratio (additional models are available from the corresponding author on request). We conclude that Group 1 HNB lavas are derived from an enriched oceanic plateau-like peridotite source region. Group 2 HNB lavas are derived from a similar source region that has been contaminated by ascending slab melts.

This conclusion helps explain the HFSE–$(SiO_2)_{8·0}$ and trace element trends in the variation diagrams of Fig. 12b–g. With regard to the HFSE–$(SiO_2)_{8·0}$ diagrams the lower $(SiO_2)_{8·0}$ and higher HFSE contents in the Group 1 lavas are the result of relatively low degrees of partial melting (~0·5–1·0%) of a mantle source not contaminated by slab components. The slightly higher $(SiO_2)_{8·0}$ and lower HFSE abundances in the Group 2 samples is the result of the mantle source being contaminated with silicic melts, and slightly higher degrees of partial melting (~1·0–2·5%). Separate garnet- and spinel-bearing OJP peridotite and 15% metasomatized mantle wedge partial melt trends are shown in the REE–

Nb variation diagrams for comparison (Fig. 12d–g). The LREE and MREE systematics of the Group 1 and 2 samples can best be described in terms of derivation from OJP-like peridotite and OJP-like mantle contaminated by slab melts, respectively. As a consequence, the elemental and isotopic trends observed in the Halberstadt data represent compositional variability arising from differing source regions and also slightly different degrees of partial melting.

Eoarchaean HNB?

Alkali basalts are rare in Archaean greenstone–TTG belts (e.g. Condie, 1994; Polat *et al.*, 1999; Hollings, 2002). Nevertheless, Nb-enriched basalts (NEB) and HNB are found in mid- to late (~2·7–3·12 Ga) Archaean provinces (e.g. Wyman & Hollings, 1998; Polat *et al.*, 1999; Wyman *et al.*, 2000, 2002; Hollings, 2002; Smithies *et al.*, 2005; Mil'kevich *et al.*, 2007). Although compositionally heterogeneous mafic rocks are present in Eoarchaean greenstone–TTG belts (e.g. Komiya *et al.*, 2004; Nutman *et al.*, 2009; Jenner *et al.*, 2013), to the best of our knowledge, NEB and HNB are absent. However, the presence of mantle-derived arc-like ultramafic dunites, island arc-like basalts and picrites and boninitic rocks in Eoarchaean strata (e.g. Polat & Hofmann, 2003; Jenner *et al.*, 2009; Nutman *et al.*, 2009; Friend & Nutman, 2011; Kusky *et al.*, 2013; Polat, 2013) suggests not only that subduction was under way from ~4·0 to 3·5 Ga, but also that subduction was not always at a low enough angle to exclude a mantle wedge.

The Halberstadt HNB are generated through small degrees of partial melting. Higher upper mantle potential temperatures in the Eoarchaean suggest that Eoarchaean upper mantle could undergo more extensive partial melting to generate primitive magmas without the incompatible element-enriched patterns seen in HNB. Figure 13h shows a basic modal batch partial melt model in which 5% of an OJP-like mantle source is contaminated with the average TTG composition from Nutman *et al.* (2009) (Supplementary Data Table C25, Appendix C). The results of 25–35% modal batch partial melting of this TTG-contaminated source can generate geochemical trends very similar to the Eoarchaean island arc data from Nutman *et al.* (2009). Interestingly, other studies present geochemical evidence that mantle source regions in the Eoarchaean could have been contaminated by slab melts (e.g. Hoffmann *et al.*, 2010). Thus, the lack of HNBs in the Eoarchaean may be the result of higher mantle temperatures generating more extensive degrees of mantle partial melting.

TECTONIC MODEL FOR GENERATING THE JTA AND HNB—AN EOARCHAEAN ANALOGUE?

The JTA and HNB model

In this section, numbers in parentheses refer to location numbers in Fig. 14. At ~55 Ma the COP is underthrusting or subducting beneath Jamaica. It has been suggested that oceanic plateaux could be resistant to subduction (e.g. Cloos, 1993), but studies from the western Pacific and the southern Caribbean provide evidence to the contrary (van der Hilst & Mann, 1994; Mann & Taira, 2004; Taira *et al.*, 2004). In the western Pacific the OJP collided with a previously SW-dipping subduction zone causing subduction to reverse its polarity. Subsequently, earthquake hypocentre transects show that the lower portions of the OJP have also begun to subduct to the SW (Mann & Taira, 2004; Taira *et al.*, 2004). Van der Hilst & Mann (1994) used seismic tomography to image the COP underthrusting South America at an angle of ~17°.

Subduction of the COP explains the generation of the Mount Hibernia and Westphalia Schists in an accretionary wedge (e.g. Abbott & Bandy, 2008). The demonstration by West *et al.* (2014) that the Mount Hibernia samples have an immobile element composition indistinguishable from that of the COP-derived Bath–Dunrobin Volcanics shows that COP material must have begun to subduct in the latest Cretaceous. Slab rollback and/or foundering of the COP lithosphere would also generate an extensional regime in the overriding plate, which can explain the Wagwater Basin.

From 30 to 50 km depth the underthrusting COP undergoes partial melting to generate JTA magmas (1). The first of these magmas ascend and metasomatize the overlying thin mantle wedge generating armoured melt pathways into the Jamaican crust. Thereafter, oceanic plateau-derived JTA melts can ascend, have limited interaction with the overlying peridotite, and finally undergo variable amphibole-dominated fractional crystallization. Simultaneously, extension in the Wagwater Basin (2) allows deeper mantle material to ascend and undergo decompression partial melting. Group 1 HNB magmas are derived from deeper melting of mantle plume-like source regions (3). Group 2 lavas are derived from decompression of metasomatized mantle wedge material (4).

Can a subducting oceanic plateau undergo partial melting?

Simple *P–T* paths for the subducting shear zone of the underthrusting COP are shown in Fig. 15a–f; full details and results are given in Supplementary Data Table C26, Appendix C. Many studies in the literature have considered highly complex *P–T* paths for deeply subducting oceanic lithosphere with a well-developed overlying mantle wedge (e.g. Van Keken *et al.*, 2002; Syracuse *et al.*, 2010). However, our underthrusting model aims to determine the temperature of a subducting oceanic plateau shear zone down to relatively shallow depths without a thick mature overlying mantle wedge. Below ~50–65 km depth the temperature of a subducting shear zone can be, and frequently is, approximated using the analytical expressions of Peacock (1992, 1996), which are in turn derived from Molnar & England (1990). Peacock (1996) demonstrated that at pressures below

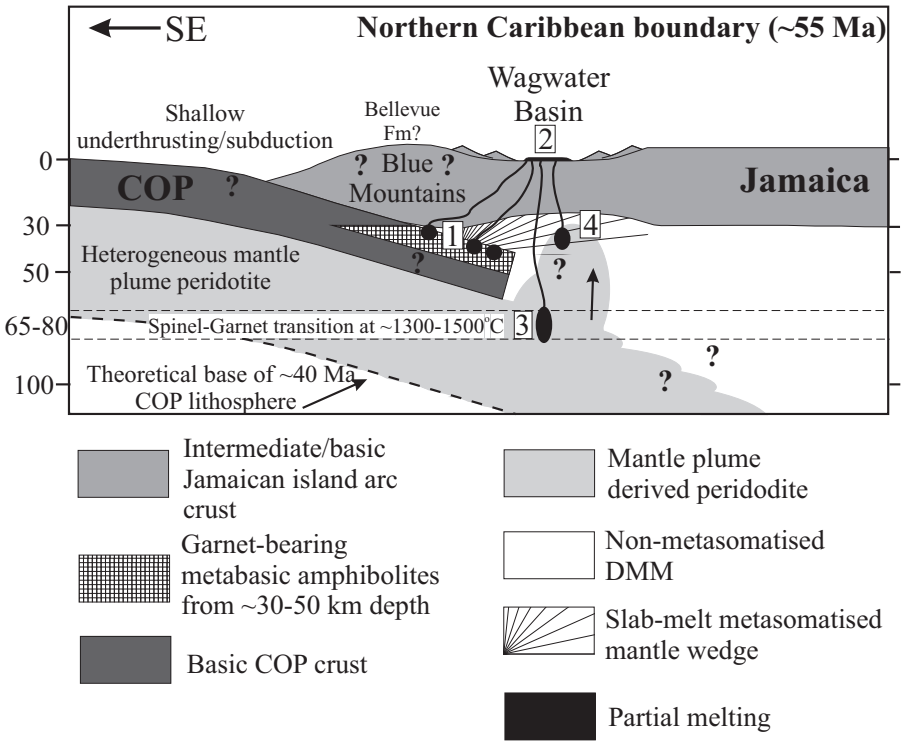

Fig. 14. Tectonomagmatic model to explain the derivation of the JTA–HNB suite of rocks in Jamaica (see text for details). Thickness of COP lithosphere at 40 Ma estimated to be ~70 km. Spinel–garnet transition estimated from Klemme & O'Neill (2000) assuming $\rho = 3300\,\text{kg m}^{-3}$; the transition will be deeper if a lower density or higher mantle temperature is used in the calculations. Location numbers are discussed in the text. Mantle thickness at [1] and just to the right of [1] is exaggerated. In reality we propose that the buoyant COP lithosphere underthrusts the Blue Mountains, but then begins to flatten after [1]. We do not show this flattening so that we can better show the processes that occur between [1] and [4].

2·1 GPa these analytical expressions generate near-identical results relative to *P–T* paths constructed using more complex numerical solutions. Thus, we use the same analytical expressions here so that our results can be easily compared with published subduction *P–T* paths at shallow depths [see Peacock (1992) for a full range of additional shallow *P–T* paths].

Our COP *P–T* paths are constructed using the most likely input parameters. These include an average convergence rate of 7·5 cm a^{-1} (Kerr & Tarney, 2005), subduction angle of 17° (Van der Hilst & Mann, 1994), thermal diffusivity of 1×10^{-6} m^2 s^{-1} (Peacock, 1996), thermal conductivity of 1·69 W m^{-1} K^{-1} (Coffin *et al.*, 2000; Frey *et al.*, 2000) and a heat flow measurement of 0·062 W m^{-2} (Anderson *et al.*, 1977). Shear stresses increase proportionally with pressure and calculations assume a density of 3000 kg m^{-3} and acceleration due to gravity of 9·8 m s^{-2}. Arguably, the two least well-known variables are convergence rate and heat flow, and these are varied in Fig. 15b–f. It should be noted that we have included shear stresses in our models so that the *P–T* paths attain higher temperatures at a given pressure with higher convergence velocities. We also recognize that estimates of shear stress vary greatly from near-zero to >100 MPa (e.g. Peacock, 1996) and, as such, we model a range of shear stresses in Fig. 15.

Figure 15a–c shows that a subducting COP shear zone will intersect the amphibole dehydration partial melt region at ~1·0–1·6 GPa, for shear stresses from just under 5% to a little over 10%, depending on convergence rate. Similarly, with a higher heat flow and convergence rates from 5–10 cm a^{-1}, the top of the COP slab will intersect the fluid-absent partial melt zone at shear stresses from just under 3·5% to a little over 7·5%. Therefore, a shallow subducting oceanic plateau can theoretically undergo partial melting to generate the JTA (and TTG-like magmas) from ~1·0 to 1·6 GPa.

Derivation of early Archaean continents: an Eoarchaean tectonic model

The upper mantle in the early Archaean (>3·5 Ga) was hotter and more fertile than today (e.g. Herzberg *et al.*, 2010; Moyen & van Hunen, 2012) and if it underwent decompression partial melting in early spreading ridges, thicker Archaean oceanic crust would be generated (e.g. Abbott *et al.*, 1994; Kerrich & Polat, 2006; Herzberg *et al.*, 2010). As a result, early Archaean oceanic crust may have been compositionally and physically similar to Mesozoic oceanic plateaux (Tarney & Jones, 1994; Kusky & Polat, 1999; White *et al.*, 1999; Smithies *et al.*, 2003, 2009; Kerrich & Polat, 2006).

Although not supported by all workers (e.g. Hamilton, 1998), many studies have proposed that the compositional and structural characteristics of rocks in early to late Archaean (e.g. ~3·8–2·5 Ga) greenstone

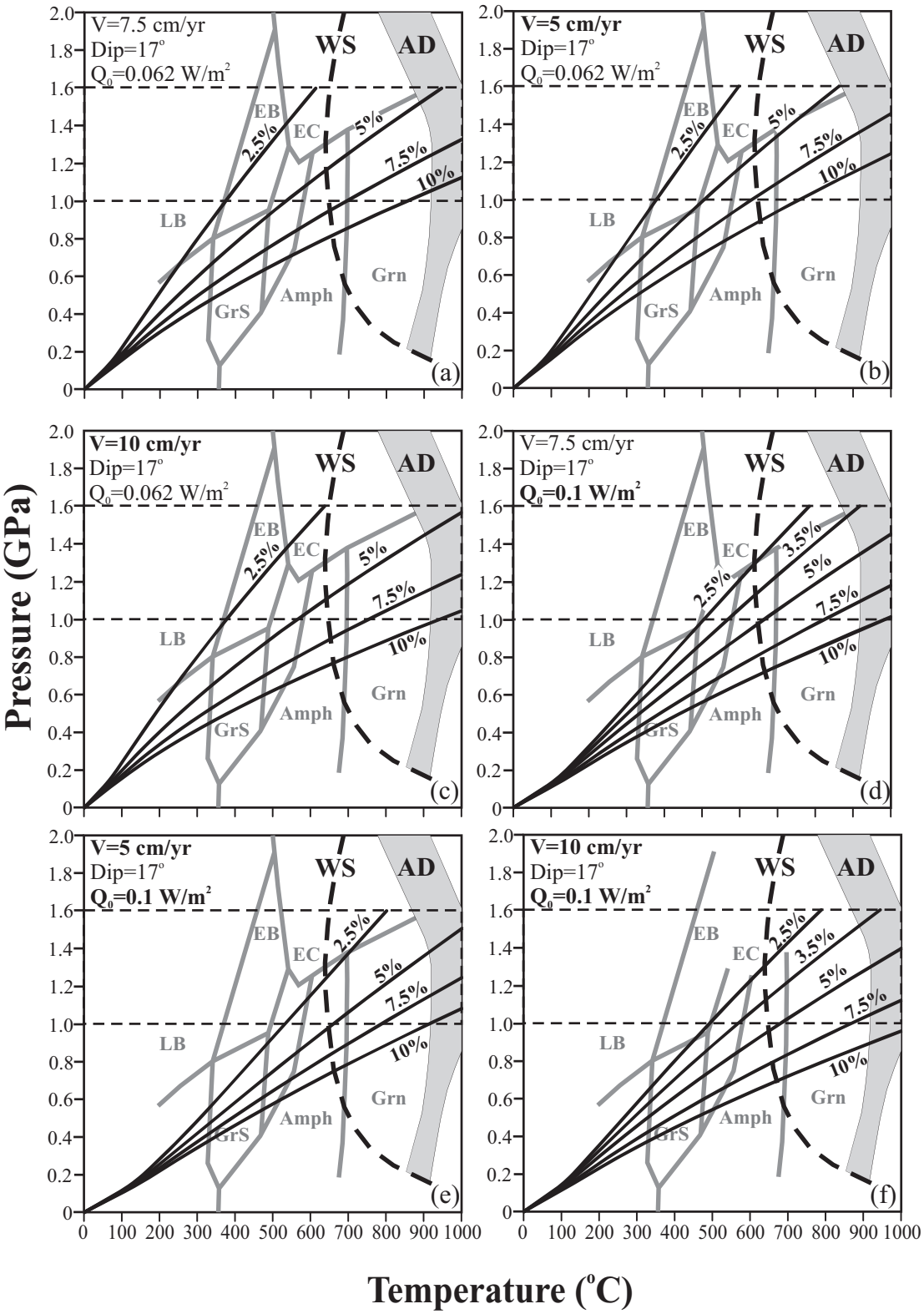

Fig. 15. Calculated *P–T* paths for a subducting COP shear zone. (a) Geothermal gradients are constructed using the most likely input parameters, which include $Q_0 = 0{\cdot}062$ W m^{-2}, $k = 1{\cdot}69$ W m^{-1} K^{-1}, $V = 7{\cdot}5$ cm a^{-1}, $\theta = 17°$, $\kappa = 1 \times 10^{-6}$ m^2 s^{-1}, $\rho = 3000$ kg m^{-3}, $g = 9{\cdot}8$ m s^{-2}. (b) and (c) use the same parameters, but V is varied from 5 to 10 cm a^{-1}. (d–f) V is varied again and Q_0 is increased to $0{\cdot}1$ W m^{-2}. Metamorphic facies and solidus information from Peacock *et al.* (1994). LB, lawsonite–blueschist facies; EB, epidote–blueschist facies; GrS, greenschist facies; EC, eclogite facies; Amph, amphibolite facies; Grn, granulite facies; WS, wet basalt solidus; AD, amphibole-dehydration partial melt zone. *P–T* paths are labelled as percentages of lithostatic pressure.

belts can be explained in terms of subduction–accretion processes (e.g. ~2·7–3·0 Ga rocks, Superior Province: Polat *et al.*, 1999; Hollings, 2002; ~2·7–2·9 Ga rocks, Baltic Shield: Mil'kevich *et al.*, 2007; 3·12 Ga rocks, Pilbara Craton: Smithies *et al.*, 2005; and ~3·7–3·8 Ga rocks of the Isua Belt, Greenland: Komiya *et al.*, 2004; Jenner *et al.*, 2009, 2013; Friend & Nutman, 2011).

The JTA are compositionally a modern analogue of Eoarchaean TTG. This suggests that, from a petrological and geochemical perspective, subduction and partial melting of oceanic plateaux (possible Eoarchaean oceanic crust) is a viable process to form the first stable continents. Therefore, we propose a model for the formation of Eoarchaean continental crust similar to the JTA–HNB subduction model shown in Fig. 14, but with the overriding Jamaican arc replaced by thick Eoarchaean mafic oceanic crust.

THE FIRST CONTINENTS AND CONCLUDING REMARKS

Using the JTA as a modern analogue we propose that Eoarchaean TTG suites can be derived by the following processes.

1. Shallow subduction and partial melting of thick Eoarchaean oceanic crust that has a similar composition to Mesozoic oceanic plateau basalt. Slab melts ascend and variably fractionate in the crust without interacting with a mantle wedge.
2. Partial melting of thick Eoarchaean subducting oceanic crust followed by interaction of the slab melts with a thin or discontinuous mantle wedge. Evidence for this interaction is obliterated by fractional crystallization of ferromagnesian minerals (mostly amphibole). Partial melting of the hot mantle wedge can subsequently generate Eoarchaean island arc basalts (seen as HNB in modern arcs).
3. Intracrustal partial melting of island arc-like and oceanic plateau-like Eoarchaean crust.

The generation of Eoarchaean TTGs and the first continents probably involved all three processes, but (3) is unlikely to be the dominant mechanism because of the low volumes of Eoarchaean island arc-like basalts. There is also a lack of oceanic plateau-like oceanic crust in the Eoarchaean rock record. However, the absence of thick Eoarchaean crust may be attributed to preservation problems because (1) the volume of present-day surviving Eoarchaean crust is tiny compared with the large continental cratons (Nutman *et al.*, 2009), and (2) early oceanic crust was subducted to generate the Eoarchaean TTG and island arc-like rocks. Thus, we propose a model for the formation of Eoarchaean continental crust similar to the model in Fig. 14, but with the overriding Jamaican arc replaced by thick Eoarchaean oceanic crust. This model is similar to those proposed by Smithies *et al.* (2003) and Martin *et al.* (2005), who suggested that Eoarchaean TTG magmas are formed by shallow partial melting of subducting slabs that underlie a very thin mantle wedge.

Melting of oceanic plateaux has also been proposed in vertical growth–basal anatexis models that do not advocate subduction zones (e.g. Bédard *et al.*, 2013; Zhang *et al.*, 2013) and our choice of mafic source region generates geochemical results similar to models that propose non-subduction environments in the Eoarchaean. Therefore, our computations can also be used to support the various vertical tectonic and crustal fusion models in the literature. However, because we use the formation of the JTA as a modern analogue for early TTG, our preferred model for generating Eoarchaean TTG suites does involve the partial melting of shallow subducting oceanic plateau-like crust. Consequently, we tentatively suggest that Eoarchaean continental generation requires potentially short-term (see van Hunen & Moyen, 2012) subduction–accretion processes.

ACKNOWLEDGEMENTS

The authors are grateful to Ali Polat, Jean Bédard and Thorsten Nagel for very constructive and patient reviews that improved the paper.

FUNDING

A.R.H. acknowledges NERC Fellowship NE/J019372/1. The funding for the radiogenic isotope work at Durham University was partly obtained via a small grant from the Centre for Earth and Environmental Science Research at Kingston University, London.

SUPPLEMENTARY DATA

Supplementary date for this paper are available at *Journal of Petrology* online.

REFERENCES

Abbott, D., Drury, R. & Smith, W. H. F. (1994). Flat to steep transition in subduction style. *Geology* **22**, 937–940.

Abbott, R. N., Jr & Bandy, B. R. (2008). Amphibolite and blueschist–greenschist facies metamorphism, Blue Mountain inlier, eastern Jamaica. *Geological Journal* **43**, 525–541.

Abbott, R. N., Jr, Jackson, T. A. & McSween, H. Y., Jr (1996). Metamorphic conditions in the Westphalia Schists of the Blue Mountain Inlier, Jamaica: Tectonic implications. *International Geology Review* **38**, 1143–1154.

Adam, J., Green, T. H. & Sie, S. H. (1993). Proton microprobe determined partitioning of Rb, Sr, Ba, Y, Zr, Nb and Ta between experimentally produced amphiboles and silicate melts with variable F content. *Chemical Geology* **109**, 29–49.

Adam, J., Rushmer, T., O'Neil, J. & Francis, D. (2012). Hadean greenstones from the Nuvvuagittuq fold belt and the origin of the Earth's early continental crust. *Geology* **40**, 363–366.

Anderson, R. N., Langseth, M. G. & Sclater, J. G. (1977). The mechanisms of heat transfer through the floor of the Indian Ocean. *Journal of Geophysical Research* **82**, 3391–3409.

Atherton, M. P. & Petford, N. (1993). Generation of sodium-rich magmas from newly underplated basaltic crust. *Nature* **362**, 144–146.

Ayabe, M., Takanashi, K., Shuto, K., Ishimoto, H. & Kawabata, H. (2012). Petrology and geochemistry of adakitic dacites and high-MgO andesites, and related calc-alkaline dacites from the Miocene Okoppe Volcanic Field, N Hokkaido, Japan. *Journal of Petrology* **53**, 547–588.

Barker, F. & Arth, J. A. (1976). Generation of trondhjemite–tonalitic liquids and Archean bimodal trondhjemite–basalt suites. *Geology* **4**, 596–600.

Barker, F., Arth, J. A., Peterman, Z. E. & Friedman, I. (1976). The 1·7- to 1·8-b.y.-old trondhjemites of southwestern Colorado and northern New Mexico: Geochemistry and depths of genesis. *Geological Society of America Bulletin* **87**, 189–198.

Bacon, C. R. & Druitt, T. H. (1988). Compositional evolution of the zoned calcalkaline magma chamber of Mount Mazama, Crater Lake, Oregon. *Contributions to Mineralogy and Petrology* **98**, 224–256.

Beard, J. S. & Lofgren, G. E. (1991). Dehydration melting and water-saturated melting of basaltic and andesitic greenstones and amphibolites at 1, 3, and 6·9 kb. *Journal of Petrology* **32**, 365–401.

Bédard, J. H. (2006). A catalytic delamination-driven model for coupled genesis of Archaean crust and sub-continental lithospheric mantle. *Geochimica et Cosmochimica Acta* **70**, 1188–1214.

Bédard, J. H., Harris, L. B. & Thurston, P. C. (2013). The hunting of the snArc. *Precambrian Research* **229**, 20–48.

Bowring, S. A., Housh, T. B. & Isachsen, C. E. (1990). The Acasta gneisses: remnant of Earth's early crust. In: Newsom, H. E. & Jones, J. (eds) *Origin of the Earth*, University Press, Oxford, 319–343.

Brown, I. & Mitchell, S. F. (2010). Lithostratigraphy of the Cretaceous succession in the Benbow Inlier, Jamaica. *Caribbean Journal of Earth Science* **41**, 25–37.

Carroll, M. R. & Wyllie, P. J. (1989). Experimental phase relations in the system tonalite–peridotite–H_2O at 15 kb; Implications for assimilation and differentiation processes near the crust–mantle boundary. *Journal of Petrology* **30**, 1351–1382.

Castillo, P. R. (2008). Origin of the adakite–high-Nb basalt association and its implications for postsubduction magmatism in Baja California, Mexico. *Geological Society of America Bulletin* **120**, 451–462.

Castillo, P. R. (2012). Adakite petrogenesis. *Lithos* **134–135**, 304–316.

Clemens, J. D., Yearron, L. M. & Stevens, G. (2006). Barberton (South Africa) TTG magmas: Geochemical and experimental constraints on source-rock petrology, pressure of formation and tectonic setting. *Precambrian Research* **151**, 53–78.

Cloos, M. (1993). Lithospheric buoyancy and collisional orogenesis: subduction of oceanic plateaus, continental margins, island arcs, spreading ridges, and seamounts. *Geological Society of America Bulletin* **105**, 715–737.

Coffin, M. F., Frey, F. A. & Wallace, P. J. et al. (2000). Site 1140. *Proceedings of the Oceanic Drilling Program, Initial Reports* **183**, 1–122.

Condie, K. C. (1994). Greenstones through time. In: Condie, K. C. (ed.) *Archean Crustal Evolution*. Elsevier, pp. 85–120.

Condie, K. (2005). TTGs and adakites: are they both slab melts? *Lithos* **80**, 33–44.

Davidson, J., Turner, S., Handley, H., Macpherson, C. & Dosseto, A. (2007). Amphibole 'sponge' in arc crust? *Geology* **35**, 787–790.

Davidson, J., Turner, S. & Plank, T. (2013). Dy/Dy*: Variations arising from mantle sources and petrogenetic processes. *Journal of Petrology* **54**, 525–537.

Defant, M. J., Richerson, P. M., de Boer, J. Z., Stewart, R. H., Maury, R. C., Bellon, H., Drummond, M. S., Feigenson, M. D. & Jackson, T. E. (1991). Dacite genesis via slab melting and differentiation: Petrogenesis of La Yeguada Volcanic Complex, Panama. *Journal of Petrology* **32**, 1101–1142.

Defant, M. J., Jackson, T. E., Drummond, M. S., De Boer, J. Z., Bellon, H., Feigenson, M. D., Maury, R. C. & Stewart, R. H. (1992). The geochemistry of young volcanism throughout western Panama and southeastern Costa Rica: an overview. *Journal of the Geological Society, London* **149**, 569–579.

DePaolo, D. J. (1981). Trace element and isotopic effects of combined wallrock assimilation and fractional crystallization. *Earth and Planetary Science Letters* **53**, 189–202.

Dessimoz, M., Müntener, O. & Ulmer, P. (2012). A case for hornblende dominated fractionation of arc magmas: the Chelan Complex (Washington Cascades). *Contributions to Mineralogy and Petrology* **163**, 567–589.

Draper, G. (1986). Blueschists and associated rocks in eastern Jamaica and their significance for Cretaceous plate-margin development in the northern Caribbean. *Geological Society of America Bulletin* **97**, 48–60.

Drummond, M. S., Defant, M. J. & Kepezhinskas, P. K. (1996). Petrogenesis of slab-derived trondjemite–tonalite–dacite/adakite magmas. *Transactions of the Royal Society of Edinburgh: Earth Sciences* **87**, 205–215.

Ewart, A. & Griffin, W. L. (1994). Application of proton-microprobe data to trace-element partitioning in volcanic rocks. *Chemical Geology* **117**, 251–284.

Faure, G. (1986). *Principles of Isotope Geology*, 2nd edn. New York: John Wiley.

Fitton, J. G. & Godard, M. (2004). Origin and evolution of magmas on the Ontong Java Plateau. In: Fitton, J. G., Mahoney, J. J., Wallace, P. J. & Saunders, A. D. (Eds) *Origin and Evolution of the Ontong Java Plateau. Geological Society, London, Special Publications* **229**, 151–178.

Fitton, J. G., Saunders, A. D., Norry, M. J., Hardarson, B. S. & Taylor, R. N. (1997). Thermal and chemical structure of the Iceland plume. *Earth and Planetary Science Letters* **153**, 197–208.

Foley, S. F., Tiepolo, M. & Vannucci, R. (2002). Growth of early continental crust controlled by melting of amphibolite in subduction zones. *Nature* **417**, 837–840.

Francis, D. & Ludden, J. (1995). The signature of amphibole in mafic alkaline lavas, a study in the Northern Canadian Cordillera. *Journal of Petrology* **36**, 1171–1191.

Frey, F. A., Coffin, M. F., Wallace, P. J., Weis, D., Zhao, X., Wise, S. W., Jr, Wähnert, V., Teagle, D. A. H., Saccocia, P. J., Reusch, D. N., Pringle, M. S., Nicolaysen, K. E., Neal, C. R., Müller, R .D., Moore, C. L., Mahoney, J. J., Keszthelyi, L., Inokuchi, H., Duncan, R. A., Delius, H., Damuth, J. E., Damasceno, D., Coxall, H. K., Borre, M. K., Boehm, F., Barling, J., Arndt, N. & Antretter, M. (2000). Origin and evolution of a submarine large igneous province: the Kerguelen Plateau and Broken Ridge, southern Indian Ocean. *Earth and Planetary Science Letters* **176**, 73–89.

Friend, C. R. L. & Nutman, A. P. (2011). Dunites from Isua, Greenland: A *ca.* 3720 Ma window into subcrustal metasomatism of depleted mantle. *Geology* **39**, 663–666.

Fujimaki, H., Tatsumoto, M. & Aoki, K.-i. (1984). Partition coefficients of Hf, Zr, and REE between phenocrysts and groundmasses. *Journal of Geophysical Research* **89**, 662–672.

Ghiorso, M. S. & Sack, R. O. (1995). Chemical mass transfer in magmatic processes. IV. A revised and internally consistent

thermodynamic model for the interpolation and extrapolation of liquid–solid equilibria in magmatic systems at elevated temperatures and pressures. *Contributions to Mineralogy and Petrology* **119**, 197–212.

Gurenko, A. A. & Chaussidon, M. (1995). Enriched and depleted primitive melts included in olivine from Icelandic tholeiites: Origin by continuous melting of a single mantle column. *Geochimica et Cosmochimica Acta* **59**, 2905–2917.

Hamilton, W. B. (1998). Archean magmatism and deformation were not products of plate tectonics. *Precambrian Research* **91**, 143–179.

Hastie, A. R. & Kerr, A. C. (2010). Mantle plume or slab window?: Physical and geochemical constraints on the origin of the Caribbean oceanic plateau. *Earth-Science Reviews* **98**, 283–293.

Hastie, A. R., Kerr, A. C., Mitchell, S. F. & Millar, I. (2008). Geochemistry and petrogenesis of Cretaceous oceanic plateau lavas in eastern Jamaica *Lithos* **101**, 323–343.

Hastie, A. R., Kerr, A. C., Mitchell, S. F. & Millar, I. (2009). Geochemistry and tectonomagmatic significance of lower Cretaceous island arc lavas from the Devils Racecourse Formation, eastern Jamaica. In: James, K. H., Lorente, M. A. & Pindell, J. (eds) *Geology of the Area between North and South America, with Focus on the Origin of the Caribbean Plate. Geological Society, London, Special Publications* **328**, 337–359.

Hastie, A. R., Kerr, A. C., Mitchell, S. F., Pearce, J. A., McDonald, I., Millar, I. & Wolstencroft, M. (2010a). Do Cenozoic analogues support a plate tectonic origin for the Earth's earliest continental crust?. *Geology* **38**, 495–498.

Hastie, A. R., Kerr, A. C., Mitchell, S. F., Pearce, J. A., McDonald, I., Millar, I., Barfod, D. & Mark, D. F. (2010b). Geochemistry and petrogenesis of rhyodacite lavas in eastern Jamaica: a new adakite subgroup analogous to early Archaean continental crust? *Chemical Geology* **276**, 344–359.

Hastie, A. R., Ramsook, R., Mitchell, S. F., Kerr, A. C., Millar, I. & Mark, D. F. (2010c). Geochemistry of compositionally distinct late Cretaceous back-arc basin lavas: Implications for the tectonomagmatic evolution of the Caribbean plate. *Journal of Geology* **118**, 655–676.

Hastie, A. R., Mitchell, S. F., Kerr, A. C., Minifie, M. J. & Millar, I. L. (2011). Geochemistry of rare high-Nb basalt lavas: Are they derived from a mantle wedge metasomatised by slab melts? *Geochimica et Cosmochimica Acta* **75**, 5049–5072.

Hastie, A. R., Mitchell, S. F., Treloar, P. J., Kerr, A. C., Neill, I. & Barfod, D. N. (2013). Geochemical components in a Cretaceous island arc: The Th/La-(Ce/Ce*) Nd diagram and implications for subduction initiation in the inter-American region. *Lithos* **162-163**, 57–69.

Hauff, F., Hoernle, K., Schmincke, H.-U. & Werner, R. (1997). A mid Cretaceous origin for the Galapagos hotspot: Volcanological, petrological and geochemical evidence from Costa Rican oceanic crustal segments. *Geologische Rundschau* **86**, 141–155.

Herzberg, C., Condie, K. & Korenaga, J. (2010). Thermal history of the Earth and its petrological expression. *Earth and Planetary Science Letters* **292**, 79–88.

Hilyard, M., Nielsen, R. L., Beard, J. S., Patiño Douce, A. & Blencoe, J. (2000). Experimental determination of the partitioning behaviour of rare earth and high field strength elements between parasitic amphibole and natural silicate melts. *Geochimica et Cosmochimica Acta* **64**, 1103–1120.

Hoffmann, J. E., Münker, C., Polat, A., König, S., Mezger, K. & Rosing, M. T. (2010). Highly depleted Hadean mantle reservoirs in the sources of early Archean arc-like rocks, Isua Supracrustal belt, southern West Greenland. *Geochimica et Cosmochimica Acta* **74**, 7236–7260.

Hoffmann, J. E., Münker, C., Næraa, T., Rosing, M. T., Herwartz, D., Garbe-Schönberg, D. & Svahnberg, H. (2011). Mechanisms of Archean crust formation inferred from high-precision HFSE systematics in TTGs. *Geochimica et Cosmochimica Acta* **75**, 4157–4178.

Hollings, P. (2002). Archean Nb-enriched basalts in the northern Superior Province. *Lithos* **64**, 1–14.

Jackson, T. A. & Smith, T. E. (1978). Metasomatism in the Tertiary volcanics of the Wagwater Belt, Jamaica. *Geologie en Mijnbouw* **57**, 213–220.

Jackson, T. A., Smith, T. E. & Isaacs, M. C. (1989). The significance of geochemical variations in Cretaceous volcanic and plutonic rocks of intermediate and felsic composition from Jamaica. *Journal of the Geological Society of Jamaica* **26**, 33–42.

Jahn, B.-M., Glikson, A. Y., Peucat, J. J. & Hickman, A. H. (1981). REE geochemistry and isotopic data of Archean silicic volcanics and granitoids from the Pilbara Block, Western Australia: implications for the early crustal evolution. *Geochimica et Cosmochimica Acta* **45**, 1633–1652.

Jenner, F. E., Bennett, V. C., Nutman, A. P., Friend, C. R. L., Norman, M. D. & Yaxley, G. (2009). Evidence for subduction at 3·8 Ga: Geochemistry of arc-like metabasalts from the southern edge of the Isua Supracrustal Belt. *Chemical Geology* **261**, 83–98.

Jenner, F. E., Bennett, V. C., Yaxley, G., Friend, C. R. L. & Nebel, O. (2013). Eoarchean within-plate basalts from southwest Greenland. *Geology* **41**, 327–330.

Jiang, M.-J. & Robinson, E. (1987). Calcareous nannofossils and larger foraminifera in Jamaican rocks of Cretaceous to early Eocene age. In: Ahmad, R. (ed.) *Proceedings of a Workshop on the Status of Jamaican Geology, Geological Society of Jamaica*. Signart Printing House, pp. 24–51.

Johnston, A. D. & Wyllie, P. J. (1989). The system tonalite–peridotite–H_2O at 30 kbar, with applications to hybridization in subduction zone magmatism. *Contributions to Mineralogy and Petrology* **102**, 257–264.

Jolly, W. T., Lidiak, E. G., Dickin, A. P. & Wu, T. W. (1998). Geochemical diversity of Mesozoic island arc tectonic blocks in eastern Puerto Rico. In: Lidiak, E. G. & Larue, D. K. (eds) *Tectonics and Geochemistry of the Northeast Caribbean. Geological Society of America, Special Papers* **322**, 67–98.

Kay, R. W. (1978). Aleutian magnesian andesites: Melts from subducted Pacific Ocean crust. *Journal of Volcanology and Geothermal Research* **4**, 117–132.

Kepezhinskas, P. K., Defant, M. J. & Drummond, M. S. (1995). Na metasomatism in the island-arc mantle by slab melt–peridotite interaction: Evidence from mantle xenoliths in the North Kamchatka arc. *Journal of Petrology* **36**, 1505–1527.

Kepezhinskas, P., Defant, M. J. & Drummond, M. S. (1996). Progressive enrichment of island arc mantle by melt–peridotite interaction inferred from Kamchatka xenoliths. *Geochimica et Cosmochimica Acta* **60**, 1217–1229.

Kerr, A. C. & Tarney, J. (2005). Tectonic evolution of the Caribbean and northwestern South America: The case for accretion of two Late Cretaceous oceanic plateaus. *Geology* **33**, 269–272.

Kerr, A. C., Aspden, J. A., Tarney, J. & Pilatasig, L. F. (2002a). The nature and provenance of accreted oceanic terranes in western Ecuador: geochemical and tectonic constraints. *Journal of the Geological Society, London* **159**, 577–594.

Kerr, A. C., Tarney, J., Kempton, P. D., Spadea, P., Nivia, A., Marriner, G. F. & Duncan, R. A. (2002b). Pervasive mantle plume head heterogeneity: Evidence from the late

Cretaceous Caribbean–Colombian oceanic plateau. *Journal of Geophysical Research: Solid Earth* **107**, paper 2001JB000790.

Kerrich, R. & Polat, A. (2006). Archean greenstone–tonalite duality: Thermochemical mantle convection models or plate tectonics in the early Earth global dynamics? *Tectonophysics* **415**, 141–165.

Klein, E. M. & Langmuir, C. H. (1989). Local versus global variations in ocean ridge basalt composition: A reply. *Journal of Geophysical Research* **94**, 4241–4252.

Klein, M., Stosch, H.-G. & Seck, H. A. (1997). Partitioning of high field-strength and rare-earth elements between amphibole and quartz-dioritic to tonalitic melts: an experimental study. *Chemical Geology* **138**, 257–271.

Klemme, S. & O'Neill, H. St. C. (2000). The near-solidus transition from garnet lherzolite to spinel lherzolite. *Contributions to Mineralogy and Petrology* **138**, 237–248.

Komiya, T., Maruyama, S., Hirata, T., Yurimoto, H. & Nohda, S. (2004). Geochemistry of the oldest MORB and OIB in the Isua Supracrustal Belt, southern West Greenland: Implications for the composition and temperature of early Archean upper mantle. *Island Arc* **13**, 47–72.

Kusky, T. M. & Polat, A. (1999). Growth of granite–greenstone terranes at convergent margins, and stabilization of Archean cratons. *Tectonophysics* **305**, 43–73.

Kusky, T. M., Windley, B. F., Safonova, I., Wakita, K., Wakabayashi, J., Polat, A. & Santosh, M. (2013). Recognition of oceanic plate stratigraphy in accretionary orogens through Earth history: A record of 3·8 billion years of sea floor spreading, subduction, and accretion. *Gondwana Research* **24**, 501–547.

LaTourrette, T., Hervig, R. L. & Holloway, J. R. (1995). Trace element partitioning between amphibole, phlogopite, and basanite melt. *Earth and Planetary Science Letters* **135**, 13–30.

Laurent, O., Doucelance, R., Martin, H. & Moyen, J.-F. (2013). Differentiation of the late-Archaean sanukitoid series and some implications for crustal growth: insights from geochemical modelling on the Bulai pluton, Central Limpopo Belt, South Africa. *Precambrian Research* **227**, 186–203.

Laurie, A. & Stevens, G. (2012). Water-present eclogite melting to produce Earth's early felsic crust. *Chemical Geology* **314–317**, 83–95.

Lewis, J. F. & Draper, G. (1990). Geological and tectonic evolution of the northern Caribbean Margin. In: Dengo, G. & Case, J. E. (eds) *The Caribbean Region. The Geology of North America, Volume H*. Boulder, CO: Geological Society of America, pp. 77–140.

López, S. & Castro, A. (2001). Determination of the fluid-absent solidus and supersolidus phase relationships of MORB-derived amphibolites in the range 4–14 kbar. *American Mineralogist* **86**, 1396–1403.

Macpherson, C. G., Dreher, S. T. & Thirlwall, M. F. (2006). Adakites without slab melting: High pressure differentiation of island arc magma, Mindanao, the Philippines. *Earth and Planetary Science Letters* **243**, 581–593.

Mann, P. & Taira, A. (2004). Global tectonic significance of the Solomon Islands and Ontong Java Plateau convergent zone. *Tectonophysics* **389**, 137–190.

Martin, H. (1999). Adakitic magmas: modern analogues of Archaean granitoids. *Lithos* **46**, 411–429.

Martin, H. & Moyen, J.-F. (2002). Secular changes in tonalite–trondhjemite–granodiorite composition as markers of the progressive cooling of Earth. *Geology* **30**, 319–322.

Martin, H., Smithies, R. H., Rapp, R., Moyen, J.-F. & Champion, D. (2005). An overview of adakite, tonalite–trondhjemite–granodiorite (TTG), and sanukitoid: relationships and some implications for crustal evolution. *Lithos* **79**, 1–24.

McDonough, W. F. & Sun, S.-s. (1995). The composition of the Earth. *Chemical Geology* **120**, 223–253.

McKenzie, D. & O'Nions, R. K. (1991). Partial melt distributions from inversion of rare earth element concentrations. *Journal of Petrology* **32**, 1021–1091.

Médard, E., Schmidt, M. W., Schiano, P. & Ottolini, L. (2006). Melting of amphibole-bearing wehrlites: an experimental study on the origin of ultra-calcic nepheline-normative melts. *Journal of Petrology* **47**, 481–504.

Mil'kevich, R. I., Myskova, T. A., Glebovitsky, V. A., L'vov, A. B. & Berezhnaya, N. G. (2007). Kalikorva structure and its position in the system of the northern Karelian greenstone belts: Geochemical and geochronological data. *Geochemistry International* **45**, 428–450.

Mitchell, S. F. (2004). Lithostratigraphy and palaeogeography of the White Limestone Group. In: Donovan, S. K. (ed.) *The Mid-Cainozoic White Limestone Group of Jamaica. Cainozoic Research* **3**, 5–29.

Mitchell, S. F. (2006). Timing and implications of Late Cretaceous tectonic and sedimentary events in Jamaica. *Geologica Acta* **4**, 171–178.

Mitchell, S. F. (2013). Stratigraphy of the White Limestone of Jamaica. *Bulletin de la Société Géologique de France* **184**, 111–118.

Mitchell, S. F. & Ramsook, R. (2009). Rudist bivalve assemblages from the Back Rio Grande Formation (Campanian, Cretaceous) of Jamaica and their stratigraphical significance. *Cretaceous Research* **30**, 307–321.

Molnar, P. & England, P. (1990). Temperatures, heat flux, and frictional stress near major thrust faults. *Journal of Geophysical Research* **95**, 4833–4856.

Moyen, J.-F. (2009). High Sr/Y and La/Yb ratios: The meaning of the 'adakite signature'. *Lithos* **112**, 556–574.

Moyen, J.-F. & Martin, H. (2012). Forty years of TTG research. *Lithos* **148**, 312–336.

Moyen, J.-F. & Stevens, G. (2006). Experimental constraints on TTG petrogenesis: implications for Archean geodynamics. In: Benn, K., Mareschal, J.-C. & Condie, K. C. (eds) *Archean Geodynamics and Environments. American Geophysical Union, Geophysical Monograph* **164**, 149–175.

Moyen, J.-F. & van Hunen, J. (2012). Short-term episodicity of Archaean plate tectonics. *Geology* **40**, 451–454.

Nagel, T. J., Hoffmann, J. E. & Münker, C. (2012). Generation of Eoarchean tonalite–trondhjemite–granodiorite series from thickened mafic arc crust. *Geology* **40**, 375–378.

Neill, I., Gibbs, J. A., Hastie, A. R. & Kerr, A. C. (2010). Origin of the volcanic complexes of La Désirade, Lesser Antilles: Implications for tectonic reconstruction of the Late Jurassic to Cretaceous Pacific–proto-Caribbean margin. *Lithos* **120**, 407–420.

Neill, I., Kerr, A. C., Hastie, A. R., Stanek, K.-P. & Millar, I. L. (2011). Origin of the Aves ridge and Dutch–Venezuelan Antilles: Interaction of the Cretaceous 'Great Arc' and Caribbean–Colombian oceanic plateau? *Journal of the Geological Society, London* **168**, 333–347.

Nutman, A. P., Bennett, V. C., Friend, C. R. L., Jenner, F., Wan, Y. & Liu, D. (2009). Eoarchaean crustal growth in West Greenland (Itsaq Gneiss Complex) and in northeastern China (Anshan area): review and synthesis. In: Cawood, P. A. & Kröner, A. (eds) *Earth Accretionary Systems in Space and Time. Geological Society, London, Special Publications* **318**, 127–154.

Patiño Douce, A. E. & Beard, J. S. (1995). Dehydration-melting of biotite gneiss and quartz amphibolite from 3 to 15 kbar. *Journal of Petrology* **36**, 707–738.

Peacock, S. M. (1992). Blueschist-facies metamorphism, shear heating, and P-T-t paths in subduction shear zones. *Journal of Geophysical Research* **97**, 17,693–17,707.

Peacock, S. M. (1996). Thermal and petrologic structure of subduction zones. In: Bébout, G. E., Scholl, D. W., Kirby, S. H. & Platt, J. P. (eds) *Subduction Top to Bottom. American Geophysical Union, Geophysical Monograph* **96**, 119–133.

Peacock, S. M., Rushmer, T. & Thompson, A. B. (1994). Partial melting of subducting oceanic crust. *Earth and Planetary Science Letters* **121**, 227–244.

Pearce, J. A. (1982). Trace element characteristics of lavas from destructive plate boundaries. In: Thorpe, R. S. (ed.) *Andesites*. Chichester: John Wiley, pp. 525–547.

Pearce, J. A. & Peate, D. W. (1995). Tectonic implications of the composition of volcanic arc magmas. *Annual Review of Earth and Planetary Sciences* **23**, 251–285.

Plank, T. & Langmuir, C. (1998). The chemical composition of subducting sediment and its consequences for the crust and mantle. *Chemical Geology* **145**, 325–394.

Polat, A. (2012). Growth of Archean continental crust in oceanic island arcs. *Geology* **40**, 383–384.

Polat, A. (2013). Geochemical variations in Archean volcanic rocks, southwestern Greenland: Traces of diverse tectonic settings in the early Earth. *Geology* **41**, 379–380.

Polat, A. & Hofmann, A. W. (2003). Alteration and geochemical patterns in the 3·7–3·8 Ga Isua greenstone belt, West Greenland. *Precambrian Research* **126**, 197–218.

Polat, A., Kerrich, R. & Wyman, D. A. (1999). Geochemical diversity in oceanic komatiites and basalts from the late Archean Wawa greenstone belts, Superior Province, Canada: trace element and Nd isotope evidence for a heterogeneous mantle. *Precambrian Research* **94**, 139–173.

Prouteau, G., Scaillet, B., Pichavant, M. & Maury, R. (2001). Evidence for mantle metasomatism by hydrous silicic melts derived from subducted oceanic crust. *Nature* **410**, 197–200.

Rapp, R. P. & Watson, E. B. (1995). Dehydration melting of metabasalt at 8–32 kbar: implications for continental growth and crust–mantle recycling. *Journal of Petrology* **36**, 891–931.

Rapp, R. P., Watson, E. B. & Miller, C. F. (1991). Partial melting of amphibolite/eclogite and the origin of Archean trondhjemites and tonalites. *Precambrian Research* **51**, 1–25.

Rapp, R. P., Shimizu, N., Norman, M. D. & Applegate, G. S. (1999). Reaction between slab-derived melts and peridotite in the mantle wedge: experimental constraints at 3·8 GPa. *Chemical Geology* **160**, 335–356.

Rapp, R. P., Shimizu, N. & Norman, M. D. (2003). Growth of early continental crust by partial melting of eclogite. *Nature* **425**, 605–608.

Reagan, M. K. & Gill, J. B. (1989). Coexisting calcalkaline and high-niobium basalts from Turrialba volcano, Costa Rica: Implications for residual titanites in arc magma sources. *Journal of Geophyical Research* **94**, 4619–4633.

Révillon, S., Arndt, N. T., Chauvel, C. & Hallot, E. (2000). Geochemical study of ultramafic volcanic and plutonic rocks from Gorgona Island, Colombia: the plumbing system of an oceanic plateau. *Journal of Petrology* **41**, 1127–1153.

Rodríguez, C., Sellés, D., Dungan, M., Langmuir, C. & Leeman, W. (2007). Adakitic dacites formed by intracrustal crystal fractionation of water-rich parent magmas at Nevado de Longaví Volcano (36·2°S: Andean Southern Volcanic Zone, Central Chile). *Journal of Petrology* **48**, 2033–2061.

Rollinson, H. (2012). Geochemical constraints on the composition of Archaean lower continental crust: Partial melting in the Lewisian granulites. *Earth and Planetary Science Letters* **351–352**, 1–12.

Rollinson, H. (2014). Plagiogranites from the mantle section of the Oman ophiolite: models for early crustal evolution. In: Rollinson, H. R., Searle, M. P., Abbasi, I. A., Al-Lazki, A. I. & Al Kindi, M. H. (eds) *Tectonic Evolution of the Oman Mountains. Geological Society, London, Special Publications* **392**, 247–261.

Rushmer, T. (1991). Partial melting of two amphibolites: contrasting experimental results under fluid-absent conditions. *Contributions to Mineralogy and Petrology* **107**, 41–59.

Sajona, F. G., Maury, R. C., Bellon, H., Cotton, J. & Defant, M. J. (1996). High field strength element enrichment of Pliocene–Pleistocene island arc basalts, Zamboanga Peninsula, Western Mindanao (Philippines). *Journal of Petrology* **37**, 693–726.

Sato, M., Shuto, K., Uematsu, M., Takahashi, T., Ayabe, M., Takanashi, K., Ishimoto, H. & Kawabata, H. (2013). Origin of late Oligocene to middle Miocene adakitic andesites, high magnesian andesites and basalts from the back-arc margin of the SW and NE Japan arcs. *Journal of Petrology* **54**, 481–524.

Sen, C. & Dunn, T. (1994a). Dehydration melting of a basaltic composition amphibolite at 1·5 and 2·0 GPa: implications for the origin of adakites. *Contributions to Mineralogy and Petrology* **117**, 394–409.

Sen, C. & Dunn, T. (1994b). Experimental modal metasomatism of a spinel lherzolite and the production of amphibole-bearing peridotite. *Contributions to Mineralogy and Petrology* **119**, 422–432.

Shaw, D. M. (1970). Trace element fractionation during anatexis. *Geochimica et Cosmochimica Acta* **34**, 237–243.

Shuto, K., Sato, M., Kawabata, H., Osanai, Y., Nakano, N. & Yashima, R. (2013). Petrogenesis of middle Miocene primitive basalt, andesite and garnet-bearing adakitic rhyodacites from the Ryozen Formation: Implications for the tectonomagmatic evolution of the NE Japan Arc. *Journal of Petrology* **45**, 2413–2454.

Smithies, R. H. (2000). The Archaean tonalite-trondhjemite-granodiorite (TTG) series is not an analogue of Cenozoic adakite. *Earth and Planetary Science Letters* **182**, 115–125.

Smithies, R. H., Champion, D. C. & Cassidy, K. F. (2003). Formation of Earth's early Archaean continental crust. *Precambrian Research* **127**, 89–101.

Smithies, R. H., Champion, D. C., Van Kranendonk, M. J., Howard, H. M. & Hickman, A. H. (2005). Modern-style subduction processes in the Mesoarchaean: geochemical evidence from the 3·12 Ga Whundo intra-oceanic arc. *Earth and Planetary Science Letters* **231**, 221–237.

Smithies, R. H., Champion, D. C. & Van Kranendonk, M. J. (2009). Formation of Paleoarchean continental crust through infracrustal melting of enriched basalt. *Earth and Planetary Science Letters* **281**, 298–306.

Springer, W. & Seck, H. A. (1997). Partial fusion of basic granulites at 5 to 15 kbar: implications for the origin of TTG magmas. *Contributions to Mineralogy and Petrology* **127**, 30–45.

Sun, S.-s. & McDonough, W. F. (1989). Chemical and isotope systematics of oceanic basalts: implications for mantle composition and processes. In: Saunders, A. D. & Norry, M. J. (eds) *Magmatism in the Ocean Basins. Geological Society, London, Special Publications* **42**, 313–345.

Syracuse, E. M., van Keken, P. E. & Abers, G. A. (2010). The global range of subduction zone thermal models. *Physics of the Earth and Planetary Interiors* **183**, 73–90.

Taira, A., Mann, P. & Rahardiawan, R. (2004). Incipient subduction of the Ontong Java Plateau along the North Solomon trench. *Tectonophysics* **389**, 247–266.

Tarney, J. & Jones, C. E. (1994). Trace element geochemistry of orogenic igneous rocks and crustal growth models. *Journal of the Geological Society, London* **151**, 855–868.

Tejada, M. L. G., Mahoney, J. J., Neal, C. R., Duncan, R. A. & Petterson, M. G. (2002). Basement geochemistry and geochronology of Central Malaita, Solomon Islands, with implications for the origin and evolution of the Ontong Java Plateau. *Journal of Petrology* **43**, 449–484.

Tiepolo, M., Oberti, R., Zanetti, A., Vannucci, R. & Foley, S. F. (2007). Trace-element partitioning between amphibole and silicate melt. In: Hawthorne, F. C., Oberti, R., Della Ventura, G. & Mottana, A. (eds) *Amphiboles: Crystal Chemistry, Occurrence and Health Issues. Mineralogical Society of America and Geochemical Society, Reviews in Mineralogy and Geochemistry* **67**, 417–452.

Tsuchiya, N., Suzuki, S., Kimura, J.-I. & Kagami, H. (2005). Evidence for slab melt/mantle reaction: petrogenesis of early Cretaceous and Eocene high-Mg andesites from the Kitakami Mountains, Japan. *Lithos* **79**, 179–206.

Turner, S., Rushmer, T., Reagan, M. & Moyen, J.-F. (2014). Heading down early on? Start of subduction on Earth. *Geology* **42**, 139–142.

Van der Hilst, R. & Mann, P. (1994). Tectonic implications of tomographic images of subducted lithosphere beneath northwestern South America. *Geology* **22**, 451–454.

Van Hunen, J. & Moyen, J.-F. (2012). Archean subduction: fact or fiction? *Annual Review of Earth and Planetary Sciences* **40**, 195–219.

van Keken, P. E., Kiefer, B. & Peacock, S. M. (2002). High-resolution models of subduction zones: Implications for mineral dehydration reactions and the transport of water into the deep mantle. *Geochemistry, Geophysics Geosystems 3*, doi:10.1029/2001GC000256.

Van Thienen, P., van den Berg, A. P. & Vlaar, N. J. (2004). On the formation of continental silicic melts in thermochemical mantle convection models: implications for early Earth. *Tectonophysics* **394**, 111–124.

Wang, O., McDermott, F., Xu, J. F., Bellon, H. & Zhu, Y. T. (2005). Cenozoic K-rich adakitic volcanic rocks in the Hohxil area, northern Tibet: lower-crustal melting in an intracontinental setting. *Geology* **33**, 465–468.

West, D. P., Jr, Abbott, R. N., Jr, Bandy, B. R. & Kunk, M. J. (2014). Protolith provenance and thermotectonic history of metamorphic rocks in eastern Jamaica: Evolution of a transform plate boundary. *Geological Society of America Bulletin* **126**, 600–614.

White, R. V., Tarney, J., Kerr, A. C., Saunders, A. D., Kempton, P. D., Pringle, M. S. & Klaver, G. T. (1999). Modification of an oceanic plateau, Aruba, Dutch Caribbean: Implications for the generation of continental crust. *Lithos* **46**, 43–68.

Willbold, M., Hegner, E., Stracke, A. & Rocholl, A. (2009). Continental geochemical signatures in dacites from Iceland and implications for models of early Archaean crust formation. *Earth and Planetary Science Letters* **279**, 44–52.

Winther, K. T. (1996). An experimentally based model for the origin of tonalitic and trondhjemitic melts. *Chemical Geology* **127**, 43–59.

Wolf, M. B. & Wyllie, P. J. (1994). Dehydration-melting of amphibolite at 10 kbar: the effects of temperature and time. *Contributions to Mineralogy and Petrology* **115**, 369–383.

Woodhead, J. D. (1988). The origin of geochemical variations in Mariana lavas: A general model for petrogenesis in intra-oceanic island arcs? *Journal of Petrology* **29**, 805–830.

Wyman, D. & Hollings, P. (1998). Long-lived mantle-plume influence on an Archean protocontinent: Geochemical evidence from the 3 Ga Lumby Lake greenstone belt, Ontario, Canada. *Geology* **26**, 719–722.

Wyman, D. A., Ayer, J. A. & Devaney, J. R. (2000). Niobium-enriched basalts from the Wabigoon subprovince, Canada: evidence for adakitic metasomatism above an Archean subduction zone. *Earth and Planetary Science Letters* **179**, 21–30.

Wyman, D. A., Kerrich, R. & Polat, A. (2002). Assembly of Archean cratonic mantle lithosphere and crust: plume–arc interaction in the Abitibi–Wawa subduction–accretion complex. *Precambrian Research* **115**, 37–62.

Yogodzinski, G. M., Kay, R. W., Volynets, O. N., Koloskov, A. V. & Kay, S. M. (1995). Magnesian andesite in the western Aleutian Komandorsky region: Implications for slab melting and processes in the mantle wedge. *Geological Society of America Bulletin* **107**, 505–519.

Yogodzinski, G. M., Lees, J. M., Churikova, T. G., Dorendorf, F., Woerner, G. & Volynets, O. N. (2001). Geochemical evidence for the melting of subducting oceanic lithosphere at plate edges. *Nature* **409**, 500–503.

Zhang, C., Holtz, F., Koepke, J., Wolff, P. E., Ma, C. & Bédard, J. H. (2013). Contraints from experimental melting of amphibolite on the depth of formation of garnet-rich restites, and implications for models of Early Archean crustal growth. *Precambrian Research* **231**, 206–217.

Ziaja, K., Foley, S. F., White, R. W. & Buhre, S. (2014). Metamorphism and melting of picritic crust in the early Earth. *Lithos* **189**, 173–184.